TABLE OF CONTENTS

Chapter 5
Global Lightning Nitrogen Oxides Production

William Koshak

5.1 The Importance of Lightning Nitrogen Oxides

The intense heating of air molecules by a lightning discharge and subsequent rapid cooling of the hot lightning channel results in the production of nitrogen oxides [Chameides, 1986]. The lightning nitrogen oxides, or "LNOx" for brevity (where NO_x = NO + NO_2), indirectly influences our climate since these molecules are important in controlling the concentration of ozone (O_3) and hydroxyl radicals (OH) in the atmosphere [Huntrieser et al., 1998; see also Crutzen 1970, 1973, 1979; Chameides and Walker, 1973; Hidalgo and Crutzen, 1977]. Analyses of Tropospheric Emission Spectrometer (TES) data show that tropical upper tropospheric ozone has the largest radiative impact [Aghedo et al., 2011]. In addition, the distribution of ozone forcing can have a substantial influence on regional rainfall patterns, even more so than its global mean annual average forcing would suggest [Shindell et al., 2012]. Since LNOx controls ozone and is the most important source of NO_x in the upper troposphere (particularly in the tropics), lightning is important to climate [see the review by Schumann and Huntrieser, 2007]. Furthermore, a substantial amount of LNOx is transported to higher latitudes via the stratosphere, extending its influence even farther [Grewe et al., 2002; Grewe et al., 2004].

Observations of lightning provide one of the most vital, simple and direct means for examining the spatial and temporal evolution of atmospheric convection across large geographic regions. The cloud buoyancy that drives vertical motions in thunderstorms results from a temperature differential on the order of only 1^oC; this means that temperature perturbations of this order are clearly important in the context of global warming [Williams, 2005].

In order to optimally track the co-varying nature of lightning and climate, and provide useful indicators that help decision makers mitigate and adapt to adverse lightning-caused impacts, it is important to employ satellite lightning data that provides not just ground flash information, but also cloud flash information. Cloud flashes outnumber ground flashes over the US by a factor of 2.94 to 1 on average [Boccippio et al., 2001], and this factor can exceed 70 for individual severe storms [Carey and Rutledge, 1998; Figure 11a]. Indeed, cloud flash information is required to fully assess lightning/climate covariance. Lightning is also uniquely coupled to thunderstorm updraft intensity (as associated with extreme weather events), and to ice precipitation based processes. Therefore, observations of lightning provide a simple and direct

means of probing and tracking changes in both convection and convective cold cloud precipitation.

Lightning nitrogen oxides affect the concentration of the greenhouse gas O_3 in the upper troposphere where climate is most sensitive to O_3. In particular, studies show that the LNOx can act to enhance O_3 [e.g., Martin et al., 2000; Edwards et al., 2003], thereby leading to atmospheric warming. Additional studies suggest that a warming climate leads to more lightning [Price and Rind, 1994; Reeve and Toumi, 1999], and hence more LNOx. Thus, a positive feedback mechanism exists: warming climate → increased frequency (and possibly intensity) of thunderstorms → increased lightning → increased LNOx → increased O_3 → warming climate (so cycle repeats). However, Williams [2005] suggests that although lightning is sensitive to temperature on many time scales, the sensitivity appears to diminish at the longer time scales. In addition, increases in cloud albedo due to increases in thunderstorm frequency/intensity would result in a cooling that would oppose the cycle. Figure 5.1 puts these and other interconnections into context, provides details on specific impacts and costs to humankind due to enhanced lightning, and thereby highlights the overall significance of LNOx.

The 3 dashed arrows in Figure 5.1 are based on laboratory results. Petersen et al. [2008] suggest that the presence of ice can increase the probability of lightning initiation (vertical dashed arrow in Figure 5.1). Peterson and Beasley [2011] found that ice helps catalyze LNO_x formation (lower horizontal dashed arrow). Additionally, Peterson and Hallett [2012] found that NO enhances ice crystal growth (upper horizontal dashed arrow).

The physical link between lightning and temperature is not only dependent on the sensitivity of convection to temperature. Detraining thunderstorm anvils act as an "ice factory" at tropopause levels and contribute to upper tropopause water vapor via sublimation [Baker et al., 1995, 1999]. Price [2000] found excellent agreement between lightning activity and upper tropopheric water vapor, which is a more important greenhouse substance than boundary layer water vapor.

Other interconnections potentially exist. First, according to the IPCC Report [1995] and Kunkel [2003], a warmer climate implies a larger number of extreme events (e.g., flash floods and severe storms that are associated with much lightning). However, Williams [2005] indicates that mean thunderstorm flash rates (a reasonable indicator of storm severity) is not larger in a warmer climate. Second, a three-fold enhancement of ground flash lightning frequency over Houston, TX has raised the issue of heat island and pollution effects [Huff and Changnon, 1972; Orville et al., 2001; Steiger et al., 2002]. Albrecht et al. [2011] provides additional connections between ground flash lightning and pollution/deforestation. Finally, increases in positive polarity ground flashes (i.e., those that deposit positive charge to the Earth's surface) have been attributed to elevated equivalent potential temperatures [William et al., 2004, 2005], and to the thunderstorm's ingestion of smoke from fires [Lyons et al., 1998; Murray et al., 2000].

Emissions of lightning nitrogen oxides are not only important in global chemistry/climate modeling, but are also important in regional air quality modeling; see for example the importance of LNOx on air pollution control problems involving tropospheric ozone [Biazar and

McNider, 1995]. The U.S. Environmental Protection Agency (EPA) Community Multiscale Air Quality (CMAQ) modeling system is applied by federal, state, local agencies and other stakeholders to evaluate the impact of air quality management practices for multiple pollutants at a variety of spatio-temporal scales. The CMAQ improves the scientific understanding and modeling capability of chemical and physical atmospheric interactions, and guides the development of air quality regulations and standards. Specifically, many state and local air quality agencies use the CMAQ modeling system to determine compliance with the National Ambient Air Quality Standards (NAAQS). At the national level, billions of dollars in emission reduction scenarios are tested using CMAQ, with an aim of determining the most efficient and cost effective strategies for attaining the NAAQS. Therefore, improvements in the LNOx emission inventory directly translate into appreciable cost savings.

5.2 Estimating Global Annual LNOx Production

5.2.1 Flash Extrapolation Method

The most common method for estimating the global annual LNOx production, the so-called *flash extrapolation method* [Lawrence, 1995], is to employ the following formula [Liaw et al., 1990]

$$G = \gamma PF \quad , \tag{5.1}$$

where G is the global lightning NO_x production per year (measured in teragrams of N per year, i.e., Tg(N)/yr), P is the average NO_x production per flash (in units of number of molecules per lightning flash), and F is the global lightning flash rate (number of flashes per second). The conversion factor γ is the ratio of the atomic mass (M = 14.0067 grams per mole) of nitrogen to Avogadro's constant (N_A = 6.02214129x10^{23} molecules per mole) times (1 Tg/10^{12} grams) times the number of seconds in a year (365.25 days/yr)(24 hrs/day)(3600 s/hr). This gives a value for γ of approximately 7.34 x 10^{-28} Tg(N) yr^{-1}/(molecule s^{-1}), where each molecule of NO or NO_2 has one atom of nitrogen).

Often in the literature, the variables G and P are defined in terms of the production of lightning NO instead of lightning NO_x. But, the difference is fairly minor. According to the chemiluminescent detector measurements of laboratory sparks made by Wang et al., [1998], it was found that in all cases the NO_x fraction was only about 5-10% greater than the NO fraction. So "lightning NO_x" and "lightning NO" are sometimes loosely used interchangeably in the literature.

Variability in G is attributable in part to the variability in P. Several estimates of P by various investigators have been summarized [Schumann and Huntrieser, 2007; Labrador et al., 2004; Lawrence et al., 1995]. These estimates were inferred in a variety of ways: theoretical, laboratory observations, field observations, and by synthesizing all or combinations of these estimates. Table 5.1 provides a summary and an update of the various values of P obtained.

The variability in P has two basic sources. First, variability occurs due to the estimation method employed. For example, laboratory sparks do not exactly simulate lightning discharges and field observations of lightning are not as nicely controlled as in a laboratory setting. Rocket triggered lightning experiments, such as in Uman et al. [1997], represent an interesting

compromise between the two extremes of a laboratory setting and field observations of nature. Second, some of the variability in the estimate of *P* is likely due to the natural variability of lightning and the thunderstorm environment in which it occurs. Clearly, lightning channel current, channel length, channel

Table 5.1. Comparison of LNO_x estimates on a per flash basis from several studies (adapted from Peterson and Beasley [2011] and Koshak et al. [2013], but expanded with additional entries from Schumann and Huntrieser[2007] and with updates for the LNOM results; see section 5.4 for a discussion of LNOM data analyses). Values with asterisks are from Schumann and Huntrieser [2007] that differed from summary values given in Lawrence et al. [1995], Labrador et al. [2004], or Peterson and Beasley [2011].

Study	Methodology	P (x 10^{25} molecules per flash)	P/N_A (moles/flash)
Noxon [1976]	Field Observations	10	166.05
Tuck [1976]	Theoretical	1.1	18.27
Chameides et al. [1977]	Theoretical	6-14	99.63-232.48
Chameides [1979]	Theoretical	16-34	265.69-564.58
Hill et al. [1980]	Theoretical	1.2, 6*	19.93, 99.63*
Dawson [1980]	Theoretical	0.8, 4*	13.28, 66.42*
Levine [1981]	Laboratory	0.5	8.30
Hameed et al. [1981]	Review & NO_y model	0.74	12.29
Kowalczyk & Bauer [1982]	Theoretical	10	166.05
Peyrous & Lapeyre [1982]	Laboratory	3.2, 2.8*	53.14, 46.50*
Drapcho et al. [1983]	Field Observations	40, (10-80)*	664.22 (166.05-1328.43)*
Borucki & Chameides [1984]	Theoretical & Lab	3.6	59.78
Bhetanabhotla et al. [1985]	Theoretical	1.6	26.57
Franzblau & Popp [1989]	Field Observations	300	4981.62
Sisterson and Liaw [1990]	Theoretical	8.2	136.16
Goldenbaum & Dickerson [1993]	Model	3.8	63.10
Lawrence et al. [1995]	Review	2.3	38.19
Kumar et al. [1995]	Field Observations	0.5, 6*	8.30, 99.63*
Ridley et al. [1996]	Field Observations	2.8-3.6	46.50-59.78
Jadhav et al. [1996]	Field Observations	6.4	106.27
Price et al. [1997]	Theoretical	6.7-67	111.26-1112.56
Huntrieser et al. [1998]	Field Observations	4-30	66.42-498.16
Wang et al. [1998]	Laboratory	3.1	51.48
Höller et al. [1999]	Field Observations	7	116.24
Stith et al. [1999]	Field Observations	1.25-12.5	20.76-207.57
DeCaria et al. [2000]	Theoretical	15.6, (14-28)*	259.05, (232.48-464.95)*
Bradshaw et al. [2000]	Review	10-20	166.05-332.11
Cook et al. [2000]	Laboratory	0.4-7.4	6.64-122.88

Table 5.1 (continued)			
Study	Methodology	P (x 10^{25} molecules per flash)	P/N_A (moles/flash)
Nesbitt et al. [2000]	Field Observations	2.67	44.34
Huntrieser et al. [2002]	Field Observations	2.7, 8.1*	44.84, 134.50*
Skamarock et al. [2003]	Model & Field Obs.	2.6	43.17
Fehr et al. [2004]	Field Observations	21	348.71
Langford et al. [2004]	Field Observations	58	963.11
Ridley et al. [2004]	Field Observations	3.2, (3.3-23)*	53.14, (54.80-381.92)*
Beirle et al. [2004]	Satellite	6	99.63
DeCaria et al. [2005]	Theoretical	27.7, (21-28)*	459.97, (348.71-464.95)*
Beirle et al. [2006]	Satellite	5.4	89.67
Rahman et al. [2007]	Field Observations	24 (10 km channel)	398.53
Ott et al. [2007]	Model & Field Obs.	21.7	360.34
Fraser et al. [2007]	Field Observations	10-33	166.05-547.98
Koike et al. [2007]	Field Observations	2-49	33.21-813.66
Schumann & Huntrieser [2007]	Review	15	249.08
Cooray et al. [2009]	Theoretical	2	33.21
Beirle et al. [2010]	Satellite	1	16.61
Ott et al. [2010]	Theoretical	30.1	499.82
Jourdain et al. [2010]	Theoretical	31.3	519.75
Bucsela et al. [2010]	Satellite	10.5	174.36
Martini et al. [2011]	Theoretical	28.9	479.90
Huntrieser et al. [2011]	Field Observations	15.1	250.74
Koshak [This Writing]	LNOM Data Analyses	13.7	227.49

altitude, and the number of strokes in a flash, all affect the amount of LNOx produced by a flash. The chemical reaction rates and scavenging processes associated with LNOx are directly tied to the chemical, microphysical, and dynamical processes associated with a thundercloud, and these properties vary from storm to storm in general. From Table 5.1, the range of estimates for P is large; i.e., from 5.0×10^{24} all the way up to 3.0×10^{27} molecules per flash.

Another source of variability in the estimate of G is the uncertainty in the estimate of the global flash rate, F. Before the launch of the first space-based lightning mappers (see section 5.5.2 below) for examining the global distribution of total (i.e., ground and cloud) flashes, the estimation of F was difficult.

An early estimate of F is attributed to Brooks [1925]. Based on available observations, he estimated the number of lightning flashes per thunderstorm and combined this estimate with a survey of global annual thunderstorm occurrence. Specifically, he estimated that there were approximately 1800 thunderstorms occurring worldwide at any given moment, each lasting about one hour and producing about 200 flashes per hour. This gives 360,000 flashes per hour, or F = 100 flashes per second, implying over 3.15 billion flashes annually.

The range of values in the global flash rate provided in Table 8.1.1 of the summary review of Lawrence et al. [1995] is 50 – 500 flashes/sec. Rakov and Uman [2003] remark that some of the variability in F is due to confusion about whether cloud or ground flashes or both are described by published flash rates, or confusion between the terms "lightning stroke" and "lightning flash."

An interesting and novel approach for inferring the global flash rate was provided by Heckman et al., [1998]. Radiation with frequencies of 5-30 Hz is ducted between the ionosphere and the surface of the Earth with little attenuation. Assuming all of this radiation is from lightning, they attempted to invert the electric and magnetic fields obtained from 10 days of observation. Their inferred average rate of vertical charge transfer squared was 1.7×10^5 (C km)^2, and by making additional assumptions about the nature of lightning, including the typical charge moments deposited in a flash, they arrived at an estimate of 22 flashes/second. This (low-end) estimate could easily be adjusted upward by "tuning" some of the assumptions made in the inversion technique.

Satellite observations of lightning provided a unique vantage point to better understand global lightning counts. A value of 123 flashes/sec was estimated by Orville and Spencer [1979] using data from two Defense Meteorological Satellite Program (DMSP) satellites; this value had a factor of 2 uncertainty. A value of 80 flashes/sec was obtained using a silicon photodiode detector on a DMSP satellite [Turman and Edgar, 1982]; this value ranged from 40 – 120 flashes/sec. Using a a set of high-frequency radio receivers on the Ionospheric Sounding Satellite-b (ISS-b) satellite, a value of 63 flashes/sec was obtained by Kotaki et al. [1981]. Data from the DMSP and ISS-b were used in conjunction with the Cloud-Ground Ratio #3 (CGR3) observations to obtain the latitudinal variation of total flash density over each major land mass and each major ocean; the information was combined in a computational model of global lightning occurrence and resulted in a value of 65 flashes/sec [Mackerras et al., 1998]. Finally, low Earth orbiting satellite lightning mappers (section 5.5.2) have provided what are considered the best estimates of F to date: 44 flashes/second [Christian et al., 2003] and a value of 46 flashes/sec [Cecil et al., 2012].

Given the variability in the estimates of F and P, the range of values 0.9 – 220 Tg(N)/yr for G reported in Labrador et al. [2004] is quite large. But, because of the advent of lightning mappers, the uncertainties in estimating F have decreased substantially. According to Fehr et al. [2004], a more likely range of G is 2-20 Tg(N)/yr. The in-depth review by Schumann and Huntrieser [2007] suggest a range of 0.6-13 Tg(N)/yr, which is based on their (2-40) x 10^{25} molecules per flash value of P, and the 44 flashes/sec global rate of Christian et al. [2003]. In any case, it appears that the primary difficulty in estimating the global production G using the flash extrapolation method is in estimating the per flash LNOx production P.

5.2.2 Thunderstorm Extrapolation Method

An alternative approach to estimating the global production of LNOx was introduced in Chameides et al. [1987]. It is based on making in-situ measurements (or inferences) of the concentration of NO_x in thundercloud anvils. The form of the estimate is

$$G = \kappa[\mathrm{NOx}]F_c S \quad , \tag{5.2}$$

where [NO_x] is the average volume mixing ratio (in units of ppbv) in the anvil produced by lightning, F_c is the average air mass flux out of the anvil (in units of g(air)/s), and S is the number of active thunderstorm cells across the globe at a given time. Here, the conversion factor $\kappa = abc$, where a is equal to the number of seconds per year times 14 g(N)/mole times 1 mole/(29 g (air)); that is, $a \approx 1.5 \times 10^7$ g(N) g(air)$^{-1}$ s yr^{-1}, b = (10^{-9}/ppbv), and $c = 10^{-12}$ Tg(N)/g(N) so that the units of G are in Tg(N)/yr. In addition, the estimate, $F_c = (v_a - v_s)\rho_a \Delta y \Delta z$ was employed by Chameides, where v_a is the horizontal wind speed *inside* the anvil, v_s is the storm system (steering level) speed taken as about half the ambient wind speed at the anvil altitude, $\rho_a \sim 500$ g(air)/m^3 is the air density in the anvil, Δy is the width of the anvil, and Δz is the depth of the anvil.

The Chameides et al. [1987] study employed (5.2) using data obtained from a NASA Convair 990 aircraft equipped to measure NO levels. The aircraft penetrated the anvils of two cumulonimbus clouds over the North Pacific Ocean. The value of [NO_x] was estimated from the NO measurements by making assumptions about the chemical conversion rates of NO to NO_2 and the associated photostationary state.

According to the review in Schumann and Huntrieser [2007], the thunderstorm extrapolation method provides a range on G between about 1-25 Tg(N)/yr. Though the method does not require knowledge of flash properties, it is difficult to estimate the true number of thunderstorms active at any one moment across the globe.

5.2.3 Global Model Fit Method

The value of G can also be inferred by adjusting the production of LNOx in a Chemical Transport Model (CTM) such that the model results best fit the aircraft measurements of trace gases that are affected by LNOx sources [Levy et al., 1996]. For example, the concentrations of upper tropospheric NO_x and NO_y (i.e., all reactive odd nitrogen or fixed nitrogen, which is any N-O combination except the very stable N_2O) are directly affected by LNOx. In addition, LNOx indirectly affects O_3, CO, HNO_3, and others, via photochemistry. According to the review by Schumann and Huntrieser [2007], systematic comparisons between LNOx-sensitive measurements and CTM results suggest a range of G between 2-8 Tg(N)/yr. However, several authors expressed doubts about the feasibility of this approach citing, for example, either missing or highly variable data (see Schumann and Huntrieser [2007; section 3.3] for additional details). Nonetheless, applications of this method using satellite observations offer important "top-down" constraints to the value of G (see section 5.5.3 of this writing).

5.3 Observations and Inferences of LNOx

In this section, and sections 5.4 and 5.5 to follow, a closer look at the variety of ways investigators have observed or inferred LNOx is discussed. This provides additional context to the difficulties associated with estimating G. Although there have been improvements in the measurements and methods for estimating P, there is still considerable debate in the lightning/chemistry community regarding what the best estimate of P should be; clearly, more work is needed to improve confidence.

To begin, some early ground-based measurements of historical importance are discussed (sections 5.3.1 and 5.3.2). Next, a few examples of field campaigns notable for their highly coordinated measurements are provided, including in situ aircraft measurements (section 5.3.3).

Finally, section 5.3.4 provides some unique insight about LNOx from artificially triggered lightning.

5.3.1 Early Examinations of Thunderstorm Rainwater

The work of von Liebig [1827] suggested that lightning contributes to the global source of NO_x. In addition, von Liebig hypothesized that the concentration of dissolved nitrate, NO_3^-, in rainwater can be explained in part by the following reactions:

$$\begin{aligned} &NO+O_3 \rightarrow NO_2 + O_2 \\ &NO_2 + OH+M \rightarrow HNO_3 + M \\ &HNO_3 \rightarrow H^+ + NO_3^- \quad , \end{aligned} \tag{5.3}$$

where the third body M is any inert molecule (e.g., N_2 or O_2), HNO_3 is the highly water-soluble nitric acid gas, and the last reaction takes place in the rainwater.

This hypothesis motivated several follow-on studies that looked for a correlation between the concentration of NO_3^- in rainwater and lightning frequency [Hutchison, 1954; Viemeister, 1960; Visser, 1961]. However, these studies found that typically only a relatively small percent of the NO_3^- was attributable to lightning. In other words, even if there were copious amounts of lightning in a region and associated lightning NO, not much of this lightning NO would show up as NO_3^- in the thunderstorm rain water. Eventually, an explanation of this result was that the conversion time (12-20 hrs) of the first two reactions in (5.3) is substantially larger than the typical (~ 1 hr) lifetime of a thunderstorm [Tuck, 1976; Chameides, 1977].

5.3.2 Clarifying Observations

The difficulties associated with examining thunderstorm rainwater clearly implied a need to find improved methods for measuring lightning nitrogen oxides. Some milestone observations in the 1970's provided substantial confirmation and clarification.

Early preliminary observations of trace nitrogen dioxide (NO_2) from lightning are provided in Reiter [1970]. The NO_2 measurements were taken at a mountain recording station 1780 meters above sea-level. A special instrument was used to measure the NO_2. It functioned on the basis of a chemical reaction that involved the oxidation of potassium iodide ions by NO_2; a current is eventually generated that is proportional to the concentration of the NO_2. The instrument had a low-end sensitivity of 0.002 mg NO_2 per cubic meter (see Reiter [1970] for additional details).

No NO_2 was detectable during times of clear air or showers, but measurable NO_2 traces were obtained during 17 thunderstorms located at or very near the recording station. Peak readings were typically 0.005 mg, but there were four cases in which peak concentrations ranged from 0.01 to 0.08 mg. Subsequently, a spectrometer was used to infer the amount of NO_2 produced by a lightning storm that occurred on July 20, 1975 [Noxon, 1976]. The spectrometer was used to scan the spectrum of the cloud deck above the Fritz Peak Observatory in the range 4300 – 4500 angstroms. This spectrum was then divided by a solar spectrum taken at small solar zenith angle. The ratio yielded a spectrum which contained atmospheric absorption features generated by the thunderstorm. It was concluded by Noxon [1976] that the local troposphere

NO_2 abundance was enhanced by a factor of 500 over the normal level due to the lightning storm, and it was estimated that there were approximately 2 x 10^{26} molecules per stroke generated. The enhancement, along with additional evidence from Noxon [1978], confirmed the tentative results in Reiter [1970].

5.3.3 Some Field Campaigns

The list of field campaigns discussed below is by no means comprehensive; i.e., see the many additional airborne-measurement-related field campaigns discussed in Table 3 of Schumann and Huntrieser [2007]. Nonetheless, the field experiments discussed here are noteworthy examples of experiments that were dedicated towards making measurements of chemical species in the inflow and outflow regions of thunderstorms in conjunction with measurements of the cloud structure, kinematics, and lightning activity. Therefore, these field campaigns are good examples of how investigators can connect chemistry measurements in the convective outflow to specific cloud and lightning characteristics.

5.3.3.1 STERAO-A

The Stratospheric-Tropospheric Experiment: Radiation, Aerosols, and Ozone (STERAO) series of field experiments was initiated to better address the complex and interdependent chemical, dynamical, electrical, and radiative processes associated with thunderstorms that directly and/or indirectly influence weather and climate [Dye et al., 2000]. The first in the series, STEREO-A, addressed deep convection and the composition of the upper troposphere and lower stratosphere. The primary objective of STERAO-A was to determine the effects of thunderstorms on the chemical structure of the middle and upper troposphere, particularly the production of LNOx, and the transport of NO_x from the boundary layer. The field experiment was conducted during the summer of 1996 in northeastern Colorado; the primary observations included (see Dye et al., [2000] for additional details):

- Colorado State University (CSU) CHILL multi-parameter Doppler radar to observe storm structure evolution.
- National Oceanic and Atmospheric Administration (NOAA) WP3D Orion aircraft for characterizing the chemical environment, including determining the entrance/exit of chemical species in the boundary layer and mid-cloud levels and storm airflow.
- North Dakota Citation jet for observing chemistry, microphysics, and airflow in or near thundercloud anvils.
- French Office Nationale d'Etudes et de Recherches Aerospatiales (ONERA) 3-D lightning interferometer for determining the location and time-of-occurrence of ground flashes.
- The National Lightning Detection Network^{TM} (NLDN) for determining the location and time-of-occurrence of ground flashes.
- The National Center for Atmospheric Research (NCAR) Atmospheric Technology Division mobile Cross-Chain Loran Atmospheric Sounding System (CLASS) for acquiring atmospheric soundings.

The STERAO-A study in Dye et al. [2000] focused on a severe storm that occurred on July 10, 1996 and that had mostly (i.e., > 95%) cloud flashes throughout most of the storm's lifecycle. They deduced that lightning contributed a minimum of 45% (and more likely 60-90%) of the total NO_x observed in the anvil.

Although it was difficult to correlate individual flashes with aircraft-measured spikes in NO mean mixing ratio, a simple model of the NO plume from lightning was introduced to estimate lightning NO production [Stith et al., 1999]. The plume model has the form

$$\lambda = b\frac{[\mathrm{NO}]p\pi D^2}{4kT} \quad , \tag{5.4}$$

where [NO] is the concentration of NO above the background (in units of ppbv), p is pressure (in Pa), T is temperature (in absolute K), D is the NO plume diameter (in meters), and λ is the resulting NO production efficiency (in molecules NO per meter of channel). The boltzmann constant is $k = 1.381 \times 10^{-23}$ m^2 kg s^{-2} K^{-1}, and as before the conversion factor is $b = (10^{-9}$/ppbv). They obtained a range from 2 x 10^{20} – 1 x 10^{22} molecules of NO per meter of lightning channel as shown in Table 5.2.

The study by DeCaria et al. [2000] performed a 2-D cloud-scale model simulation of the STERAO-A storm that occurred on July 12, 1996. One of their objectives was to infer from the simulations and available measurements the relative production of NO_x by ground and cloud flashes. Defining P_g to be the NO_x production per ground flash, and P_c the NO_x production per cloud flash, they estimated that P_g should be in the range 200-500 moles and that the model results agree best with the observations when the ratio P_c/P_g is in the range 0.5 – 1. See subsection 5.5.4.1 for additional estimates of this ratio.

Three-dimensional cloud scale chemical transport models have also been developed and applied to STERAO-A storms [e.g., Skamarock et al., 2000; Stenchikov et al. 2005]. DeCaria [2005] applied the Stenchikov et al. [2005] model to again examine lightning NO_x production in the July 12, 1996 storm (as well as trace gas transport and photochemical ozone production). In their analysis, they concluded that the values $P_g = P_c = 460$ moles give the best reproduction of the observed mixing ratios and shape of the anvil NO_x plume.

5.3.3.2 EULINOX

The European Lightning Nitrogen Oxides (EULINOX) field experiment was coordinated by the Deutsches Zentrum für Luft- und Raumfahrt (DLR) located near Munich, Germany and conducted in July 1998 [Höller and Schumann, 2000]. An important objective of the experiment was to estimate the importance of LNOx in comparison to other sources of NO_x; there was a desire to reduce the uncertainties involved in both the production and effect of LNOx from the flash scale to the synoptic scale. The idea was that an improved understanding of the relevant processes on the small scale is necessary for a better representation of the effects on the larger scale. An important specific question asked by the EULINOX project was, "Can one deduce the LNOx source per flash, or per thunderstorm, from the planned observations?".

Two DLR aircraft were used to make in-situ chemical, particle and meteorological measurements: a Dornier-228 turboprop completed measurements in the boundary layer, and a Falcon jet made measurements primarily in the upper troposphere. Both aircraft were equipped with instruments for measuring NO, ozone, and carbon dioxide, and the Falcon jet additionally measured NO_2, other chemical and particle measurements, and some standard data (position, altitude, temperature, humidity, pressure, and the 3 components of the wind field) [Huntrieser et al., 2002]. The Falcon completed several flights over much of central Europe, whereas the

Dornier-228 completed fewer flights and covered a region more local to the DLR operation center in Oberpfaffenhofen, Germany.

For lightning observations, the ONERA VHF interferometric lightning mapper was used to locate the fast streamer processes in ground and cloud flashes; 3-D reconstruction of flash channels was possible within about 50 km of the DLR operation center and 2-D channel location was possible for flashes within about 100 km [Fehr et al., 2004]. Two Lightning Position and Tracking System (LPATS) [Casper and Bent, 1992] sensors were employed to obtain 2-D locations of ground flashes. NASA satellite lightning observations from the Optical Transient Detector (OTD; 1999-2000, see section 5.5.2) were also available for EULINOX.

In addition, several other measurements were available for EULINOX. Radar data included: DLR Polarization Diversity Radar (POLDIRAD) polarimetric doppler radar, and data from the German Weather service doppler/reflectivity radars. Sounding data (profiles of pressure, temperature, humidity) and mesonet data (surface pressure, temperature, humidity, wind) were available. Finally, EULINOX benefitted from a variety of additional satellite observations (infrared, visible, WV images, ozone, NO_2). See [Höller and Schumann, 2000] for additional details.

For an average EULINOX thunderstorm, ~70% of the anvil NO_x was produced by lightning and ~30% was transported from the boundary layer; the amount of LNOx was found to exceed 80% in larger EULINOX thunderstorms [Huntrieser et al., 2002]. The Huntrieser et al. [2002] study found that the maximum NO mixing ratio measured inside a thundercloud near lightning was 25 ppbv. In addition, they employed the thunderstorm extrapolation method (equation (5.2) of section 5.2.2) to estimate the annual global LNOx production G. They assumed the values: $S \sim 2000$, and $F_c \sim 1.05 \times 10^{11}$ g(air)/s, where $(v_a - v_s) \sim 7$ m s^{-1}, $\rho_a \sim 500$ g/m^3, $\Delta y \sim 30{,}000$ m, and $\Delta z \sim 1000$ m. They used the estimate anvil $[NO_x] \sim 0.9$ ppbv, where the value 0.9 ppbv represented the average of all EULINOX cases. From (5.2) they obtained $G \sim 3$ Tg(N)/yr. [They also applied the simple plume model given in equation (5.4) and obtained 2.7×10^{21} molecules NO per meter of channel. This gave $G \sim 4$ Tg(N)/yr when an ONERA interferometer-derived channel length of 30 km was used in conjunction with an assumed global flash rate of 65 s^{-1}.]

A 3-D cloud model, with LNOx emissions represented by a Lagrangian particle approach, was applied to study the EULINOX supercell storm that occurred on July 21, 1998 [Fehr et al., 2004]. The simulation used both parameterized and observed ground and cloud flash frequencies. Experimentally deduced values for the ground flash NO_x production of 4.9 kg(N), or equivalently 2.1×10^{26} molecules NO (348.7 moles) and a ratio between cloud and ground NO_x production of 1.4 were confirmed by the model. The ratio of 1.4 is substantially larger than the ratio of 0.1 initially assumed by Price et al. [1997].

5.3.3.3 TROCCINOX

During February-March 2004 and February 2005, airborne in-situ measurements of NO, NO_y, CO, and O_3 mixing ratios, $J(NO_2)$ photolysis rate, and meteorological variables were obtained in the anvil outflow of thunderstorms over southern Brazil as part of the Tropical Convection, Cirrus and Nitrogen Oxides Experiment (TROCCINOX) field experiment [Schumann et al., 2004; Huntrieser et al. 2007; Schumann and Huntrieser 2007]. The NO_2 (and NO_x) mixing ratios were inferred from the measurements of NO, O_3, $J(NO_2)$, pressure, and temperature by assuming a photostationary steady state. The airborne measurements were carried

out using the DLR Falcon aircraft (maximum flight altitude of 12.5 km), and also in part with a high altitude (~ 20 km) Russian M55 Geophysica aircraft. During this wet season, both subtropical and tropical thunderstorms were investigated. In addition to ancillary satellite and radar information, lightning observations in southern Brazil were obtained using a six station VLF/LF lightning detection network (LINET) developed by the University of Munich [Betz et al., 2004; Betz et al., 2007], the operational Brazilian network RINDAT (Rede Integrada Nacional de Detecção de Descargas Atmosféricas), and satellite Lightning Imaging Sensor (LIS; 1997-present, see section 5.5.2).

The composition of the anvil outflow from a large, long-lived Mesoscale Convective System (MCS) was, for the first time, investigated [Huntrieser et al, 2007]. The MCS, which had advected from northern Argentina and Uruguay, was found to have significantly enhanced NO_x, CO and O_3 mixing ratios. From the penetrations of TROCCINOX thunderstorms, Huntrieser et al. [2007] found that NO_x mixing ratios in the anvil outflow region between 8 – 12.5 km were enhanced with average mixing ratios varying between 0.2 and 1.6 nmol mol^{-1}, or ppbv. They estimated that the NO_x from the anvil outflow of a subtropical thunderstorm was about 80% due to lightning, and only a minor contribution from the boundary layer.

Correlating the spatial distribution of measured anvil NO_x enhancement with individual lightning flashes is difficult. To help, the distribution of LNOx in and near thundercloud cells was simulated with the Lagrangian particle dispersion model FLEXPART. Huntrieser et al. [2008] found that the amount of nitrogen produced by lightning in a thunderstorm is not well correlated with the number of (LINET) strokes; they stated that stroke length, peak current, and release height also need to be considered. Nonetheless, they estimated that the average LNOx per LIS flash was ~1 and ~ 2-3 kg(N) for three tropical and one subtropical Brazilian thunderstorms, respectively. Consequently, they suggested that tropical flashes may be less productive than subtropical flashes. With these values and an assumed global flash rate of 44 flashes/sec, they estimated mean values of *G* of 1.6 and 3.1 Tg(N)/yr, for the respective storms mentioned.

Finally, the study by Höller et al. [2009] asserted that the effective lightning stroke length is the dominant factor for LNOx production, and that stroke peak current and emission height were less significant.

5.3.4 Rocket Triggered Lightning

By launching a small (~ 1 meter) plastic or steel rocket with a trailing wire, either grounded or ungrounded, into a thundercloud, it is possible to artificially trigger a lightning discharge. This so called *rocket-and-wire* technique is described in Rakov and Uman [2003]. The trailing wire is composed of copper or steel and has a diameter of ~ 0.2 mm; it is spooled out either from the ground or from the rocket.

The first rocket-triggered lightning occurred in 1960 from a research vessel situated off the west coast of Florida [Newman, 1965]; the study employed grounded trailing wires. The first triggering over land occurred in 1973 in Saint Privat d'Allier, France [Fieux et al., 1975]. In addition to the triggered-lightning program developed in France, other triggered-lightning programs were developed in Japan (Kahokugata, Hokuriku coast, Okushishiku), the US (New Mexico, Florida, Alabama), China (multiple sites over the northern and southeastern regions), and Brazil (Cachoeira Paulista).

One of the triggered-lightning programs in Florida was developed in 1993 in Camp Blanding [Uman et al., 1997] and is presently still operational. It has been found that the

characteristics of the leader-return-stroke sequences in triggered-lightning are similar in most, if not all, respects to the *subsequent* leader-return stroke sequences in natural ground flashes [Rakov and Uman, 2003; Depasse, 1994]. Evidently, the first leader-return stroke sequence in a natural ground flash is not as well represented by triggered-lightning.

Acknowledging the fact that triggered-lightning is not exactly the same as natural lightning, one can still attempt to make measurements of triggered-lightning NOx (TLNOx) as a proxy to LNOx. An obvious benefit of such an approach is that one controls where and when the discharge will occur, so that the placement and operation of chemistry measurements are optimized. In addition, one can also isolate a section of the triggered-lightning channel in a given volume so that no assumptions have to be made about the wind velocity or the dispersion of NO_x from the channel.

In July 2005 at the Camp Blanding, Florida triggering site; i.e., the International Center for Lightning Research and Testing (ICLRT), Rahman et al. [2007] obtained the first direct measurements of TLNOx. Three negative lightning flashes were triggered using the rocket-and-wire technique. Two electrodes were used; one was connected to the rocket launcher where the lightning channel terminates, and the other electrode was grounded. The separation distance between the electrodes was 3 cm, and they were placed within a cylindrical chamber. The apparatus effectively isolated a 3 cm section of channel. Atmospheric air entered the chamber continuously, and evacuated air from the chamber passed through a calibrated NO_x Analyzer (model 9841B, Monitor Labs).

Although the number of triggered lightning was small, they concluded that relatively slow discharge processes, those occurring on time scales of milliseconds to hundreds of milliseconds (such as continuing currents in ground flashes), can contribute significantly to NO_x production. Moreover, they asserted that the return strokes within a ground flash are not the primary producers of NO_x; i.e., their data showed that the NO_x production is primarily from long-duration, steady currents, as opposed to microsecond-scale impulsive return stroke currents. Since cloud flashes transfer large amounts of charge via steady currents on the order of 100 A, the implication was that cloud flashes could be as (or more) efficient at producing NO_x than ground flashes [Rahman et al., 2007].

Overall, the Rahman study found a production of 2.0×10^{22} NO_x molecules per meter of channel for one triggered flash, and 2.4×10^{22} molecules per meter for each of the other two triggered flashes. The value of $P = 24 \times 10^{25}$ molecules/flash expressed in Table 5.1 was based on the latter value, and it was arbitrarily multiplied here by a 10 km channel length for order-of-magnitude purposes only. The value of 10 km is an underestimate (see following section regarding channel length estimation based on VHF lightning mapping data).

5.4 The Lightning Nitrogen Oxides Model (LNOM)

The previous section discussed various conventional methods for estimating the amount of nitrogen oxides produced by a flash. In this section, a more recent method for estimating LNOx is discussed. The approach is based on a research-grade software package, named the Lightning Nitrogen Oxides Model (LNOM), which was developed at the NASA Marshall Space Flight Center (MSFC). The LNOM analyzes multiple lightning datasets in order to make detailed estimates of LNOx on a flash-by-flash basis. As such, LNOM data analyses represent the most detailed "bottom-up" constraints on the value of P in equation (5.1).

5.4.1 Motivations

Given the importance of LNOx in global climate studies as discussed in section 5.1, the ability to accurately model LNOx production within global climate models is paramount. For example, in the NASA Goddard Institute for Space Studies (GISS) ModelE2 global climate model [Schmidt et al., 2006] the parameterization employed is based on the study by Price et al., [1997] which describes LNOx production from a single flash as follows:

$$P = EY \, . \tag{5.5}$$

Here, E is the estimated mean *energy* of the flash (Joules per flash), Y is the *yield* (# molecules of NO_x per Joule), and so P is the estimated average amount of NO_x *production* per flash (# molecules of NO_x per flash). As mentioned above, most of the NO_x yield (~ 90% or more) is in the form of NO [Wang et al., 1998]. Price et al. [1997] arrived at the estimates: $E \sim 6.7 \times 10^9$ J (for ground flashes), $E \sim 6.7 \times 10^8$ J (for cloud flashes), and $Y \sim 10^{17}$ molecules/J.

Note that equation (5.5) pertains only to the *LNOx production per flash* portion of the actual parameterization provided in Price et al. [1997; equation (15)] which includes various temporal and molecular weight conversion factors and flash count information that are not pertinent to the present discussion. In addition, GISS multiplies the Price et al. [1997] production parameterization by their own tuning factor, called `tune_NOx` in the ModelE2 code, in an attempt to improve results.

The estimates of E and Y are simply coarse educated guesses, or so called "back of the envelope" calculations based on reasonable syntheses of the appropriate lightning literature. Moreover, one should recognize that the production parameterization in (5.5) provides only two numbers: the production P_g from ground flashes and the production P_c from cloud flashes. In reality, the production is not fixed for all ground flashes or for all cloud flashes. Presently, these fixed values are being applied within ModelE2 in conjunction with the flash count parameterization (discussed later) to arrive at the total LNOx source.

By today's standards, the Price et al. [1997] estimates are overly simplistic since we now have advanced, ground-based lightning detection systems capable of deeply probing the nature of lightning flashes, and accumulating realistic distributions of their properties that are critical for making accurate estimates of LNOx production. In particular, the bulk and estimative parameterization in equation (5.5) glosses over many important variables that can now be accounted for in part, or fully:

- Variable lightning channel lengths (longer channels → more LNOx).
- Variable lightning currents (larger currents → more energy → more LNOx).
- Variable lightning channel altitude (lower altitude → higher air density → more LNOx). That is, the yield Y in equation (5.5) is actually altitude dependent not a fixed constant (see Chameides [1986; equation (6.2)], and Wang et al. [1998; equation (9)]).
- Variable # of return strokes in ground flashes (more strokes → more LNOx).
- Variable production physics (i.e., certain physical processes, if they occur in a flash, would produce additional LNOx [see Cooray et al., 2009].

In addition, there are deficiencies in the flash count parameterizations. For example, to calculate the number of ground and cloud flashes in each ModelE2 grid box, NASA GISS presently applies a parameterization described in Price and Rind [1992, 1993, 1994], and Price et al., [1997] that has the following form:

$$
\begin{aligned}
f_g &= \alpha \left[qH^p \right] \qquad \text{(\# ground flashes per minute)} \\
f_c &= (1-\alpha) \left[qH^p \right] \qquad \text{(\# cloud flashes per minute).}
\end{aligned}
\tag{5.6}
$$

The quantity in square brackets [qH^p] is the *total lightning flash rate f* (# flashes/min), where H is the cloud top height in kilometers. The empirical constants q and p depend on whether it is a continental thunderstorm (q = 3.44 x 10^{-5}, p = 4.90) or a maritime thunderstorm (q = 6.40 x 10^{-4}, p = 1.73). The variable $\alpha = (aD^4+bD^3+cD^2+dD+e)^{-1}$ is the *ground flash fraction* (i.e., the proportion of ground flashes in an individual thunderstorm), where D is the *cold cloud thickness* in kilometers (i.e., the vertical thickness between the altitude of the 0°C isotherm and cloud-top height). The empirical constants are: a = 0.021, b = -0.648, c = 7.49, d = -36.54, and e = 64.09.

GISS applies their own tuning factors (one for continental storms, and one for maritime storms) in an attempt to improve the parameterizations. Moreover, the values of the constants q and p have been adjusted over the years to drive the geographical distribution of ModelE2 lightning frequencies as close as possible to NASA Optical Transient Detector (OTD) lightning observations (see model/observation comparisons provided in Plate 2 of Shindell et al. [2001], Figure 8 of Shindell et al. [2003], and Figure 11 of Shindell et al. [2006]). Despite these improvements, there are still several shortcomings which need to be addressed:

a) *Documented Deficiencies:* ModelE2 tends to overestimate lightning over SE Asia and Indonesia, and this leads to overestimates of the total flashes of 5% during boreal summer and 17% during boreal winter; overestimates are pronounced over South America during the boreal winter [Shindell et al., 2006].

b) *Separate Verification Needed:* Comparisons of ModelE2 flash frequency with OTD data are fundamentally incomplete because OTD only provides the total flash number (i.e., the sum of both ground and cloud flashes). Since the parameterizations in (5.6) provide both ground flash and cloud flash counts, it is important to separately verify the accuracy of each of these parameterizations, particularly since the typical amount of LNOx produced per ground and per cloud flash could differ.

c) *Low Detection Efficiency:* OTD was a prototype sensor that had daytime and nighttime flash detection efficiencies of only 44% and 56%, respectively [Boccippio et al., 2002]. In addition, the limited view-time associated with its low Earth orbit required that one perform 55 day sampling strategies in an attempt to alleviate biases associated with the diurnal cycle of lightning. Even though the Lightning Imaging Sensor (LIS) offers higher detection efficiency and better location accuracy, it only covers the tropics, and like OTD, does not discriminate between ground and cloud flashes. Therefore, an high detection efficiency, <u>*continuous*</u> monitoring system that detects (and discriminates between) ground and cloud flashes is needed to fully investigate the accuracy of the parameterizations in (5.6).

d) *Limitations Associated with Ground Flash Fraction:* The polynomial expression given above for the ground flash fraction α is only based on 139 thunderstorms which occurred

only in the summer and only over the US [Price and Rind, 1993], yet is being applied globally and seasonally within the ModelE2. In addition, the value of D in the parameterization is restricted to the range 5.5 km < D < 14 km.

e) *Theoretical Inconsistencies:* The parameterization for total flash rate in maritime thunderstorms contains a formal derivational inconsistency and predicts nonphysical cloud-top heights when the parameterization is inverted [Boccippio, 2002].

5.4.2 Functionality

Since lightning has highly variable channel lengths, currents, altitudes, and stroke number, and since there are a variety of discharge types within a flash that produce different amounts of LNOx, it is crucial that the variability of lightning be addressed to obtain accurate estimates of LNOx production, including its vertical profile. This implies that a very large number of flashes should be analyzed on a flash-by-flash basis (using the appropriate lightning detection technologies and data analysis techniques) so that quantitative and realistic statistical distributions of LNOx production can be obtained.

In order to accomplish these objectives, the LNOM was developed [Koshak et al., 2009, 2010, 2011; Koshak and Peterson, 2011; Koshak et al., 2013]. The LNOM implements a realistic description of lightning while at the same time combines useful laboratory findings with state-of-the-art lightning observations to obtain accurate LNOx estimates of individual flashes.

Figure 5.2 provides an overview of the basic function of the LNOM. It ingests VHF lightning channel mapping data such as obtained from the North Alabama Lightning Mapping Array [NALMA; Koshak et al., 2004]. The VHF data provide remarkable information about the spatial and temporal evolution of the lightning channel; over the LNOM analysis region the VHF data provides 4D channel mapping with a location accuracy measured in tens of meters and with a time resolution of 80-100 μsec [Thomas et al., 2004]. The LNOM also ingests ground flash data from the National Lightning Detection Network^{TM} (NLDN, Cummins et al., 2006; Cummins and Murphy, 2009]. Note that the focus of LNOM is on the production of NO_x, not its subsequent chemical conversion, transport (convective, advective), or removal (e.g., wet scavenging).

In summary, the LNOM analyzes each flash individually by examining the VHF and NLDN data associated with the flash. It performs the following basic processing steps:

1. *Flash Typing:* Based on the VHF and NLDN data, LNOM categorizes the flash as either a ground flash or a cloud flash; this is an important initial step because many physical processes associated with LNOx production depend on flash type.

2. *Channel Length Computation:* LNOM spatially averages the VHF data, and computes the total channel length.

3. *Channel Chopping:* LNOM dices up the lightning channel into 10-meter segments, and stores both the orientation and 3D location of each of these segments.

4. *NO_x Computation:* LNOM applies algorithms to compute the LNOx from each 10-meter segment based on empirical and theoretical formulas provided in Wang et al., [1998] and

Cooray et al. [2009]. These algorithms account for many physical mechanisms that produce NO_x, and the algorithms are only applied if the mechanism is present. For example, ~75% of positive polarity ground flashes are associated with *continuing currents*, but only about 30% of negative polarity ground flashes contain such currents. Similarly, 10-meter segments that are a part of a ground flash channel, but that are not located within the channel(s) to ground (i.e., are not associated with the return stroke) would not be associated with return stroke NO_x production. LNOM accounts for these and other nuances. Because of the arbitrary geometrical orientation and altitude of the individual 10-meter lightning channel segments, several of the formulas for computing LNOx provided in Wang et al., [1998] and Cooray et al., [2009] are appropriately generalized within the LNOM computational algorithms. The production mechanisms accounted for by LNOM include the following:

a. NO_x production from return strokes [based on Wang et al. 1998]:
   - accounts for peak current magnitude using NLDN data
   - accounts for the number of strokes in the flash using NLDN data
   - accounts for air density (channel segment altitude) using VHF data

b. NO_x production from processes other than return strokes [Cooray et al., 2009]:
   - production from the hot core of stepped leaders
   - production from stepped leader corona sheath
   - production from the hot core of dart leaders
   - production from K-changes
   - production from continuing currents and associated M-components

5. *LNOM Data Product Creation:* Based on all these computations, the LNOM creates the final LNOM data products, typically for monthly, annual, or multi-annual analysis periods within the LNOM analysis domain (see right-hand boxes in Figure 5.2 and further description to follow).

The standard LNOM analysis domain is a fixed (i.e., Eulerian) cylinder, having a height range extending from the surface to 20 km, and having a horizontal radial range of 20.31km. This radius was chosen since it produces the areal equivalent of a 36km x 36km Community Multiscale Air Quality (CMAQ) grid cell; i.e., an initial application of the LNOM was for improving CMAQ air quality forecasts. The LNOM cylinder dimensions can be adjusted as needed for other applications.

In fact, the most recent applications of the LNOM, still being conducted at the time of this writing, involve a Lagragian LNOM analysis domain cylinder that moves with individual storms or storm complexes to track LNOx production. In these applications, the period over which the LNOM products are produced is much shorter; i.e., on the order of the duration of a thunderstorm cell, rather than the much longer monthly or annual periods mentioned above. This effort is being lead by researchers at the University of Alabama – Huntsville (UAH), the Universities Space Research Association (USRA), and NASA MSFC as part of the Deep Convective Clouds and Chemistry Experiment (DC3; http://www.eol.ucar.edu/projects/dc3/).

5.4.3 Data Products

There are several LNOM output data products, including: channel length distribution (CLD), segment altitude distribution (SAD), vertical LNOx Production Profile (LNPP), and LNOx Distribution (LND). These are provided for ground flashes alone, for cloud flashes alone, and for all flashes. The ancillary products shown in Figure 5.2 are primarily for research purposes; for example, the Channel Connection Diagram (CCD) is an ancillary product used to visually evaluate the accuracy of the LNOM channel computation module. It provides various cross-sectional plots of the VHF sources for an individual lightning flash, the linear connections made between the spatially averaged and filtered sources, and the resulting channel length computation.

The SAD provides the number of 10-meter channel segments in each 100-meter altitude interval of the LNOM analysis cylinder during a prescribed LNOM analysis time period. This product gives the user an idea of how much LNOx might be expected in a certain vertical layer of the atmosphere during a given period just due to the amount of lightning activity in that layer and/or due to the occurrence of some relatively long channel discharges in the layer. The left panel in Figure 5.3 provides an example of the SAD product for an air quality study in [Koshak et al., 2013], the LNOM analysis period for this SAD is one month.

Figure 5.3 (right panel) shows an example of the LNPP data product. It is important to note that the LNPPs are not dynamically mixed profiles, but are strictly production profiles. Therefore, they provide insight and guidance on how best to modify the baseline "C shape" LNOx profile due to Pickering et al. [1998] that was employed by ModelE2. For example, the LNOM profiles more closely resemble "backward C-shapes," which suggests that cloud dynamics do not "reverse" the basic LNOx source profile, but rather just smooth it out in the vertical. Similarly, backward C-shaped profiles were found in Ott et al. [2010; Table 2].

The LND is a frequency distribution of the LNOx. So given $N = N_g + N_c$ flashes analyzed by the LNOM, where N_g is the number of ground flashes and N_c is the number of cloud flashes, the ground and cloud flash LNOx frequency distributions can be denoted as $\Phi(p_g)$ and $\Phi(p_c)$, respectively. Here, p_g is the independent variable for ground flash LNOx, and p_c is the independent variable for cloud flash LNOx. Since the LNOM analysis domain has a finite radial range, it is always possible to truncate flashes that cross the vertical cylindrical wall of the LNOM domain. However, the LNOM keeps track of those flashes that are truncated, and additionally computes the LNOx produced by the portion of the channel outside the cylinder wall. Hence, the total LNOx from each flash is calculated and this stored information allows LNOM to generate the LND product.

5.4.4 Data Archive

At the time of this writing, the LNOM data archive presently contains LNOx analyses for 468,928 flashes. Most of these flashes are derived from 9 years (2004-2012) of North Alabama thunderstorms. The remaining flashes are from 4 years of data derived from the DC metropolitan LMA network.

Figure 5.4 provides the channel length distributions (CLD product) for the entire 9 years of North Alabama thunderstorms; this corresponds to a total of 404,197 flashes. The distribution of channel length is given for all flashes, for just cloud flashes, and for just ground flashes. Again, the CLDs can be generated for any analysis time period desired (e.g., CLDs associated for just the 1 month time period given in Figure 5.3 are obtainable by the LNOM). Note from

Figure 5.4 that the mean channel length for ground flashes is about 66.9 km, whereas the mean channel length for cloud flashes is about 47.6 km. Longer channel length implies more NO_x production, all else being equal. In addition, more of the ground flash channel is at lower altitude (higher air density) than the cloud flash channel, so in the case of ground flash channel there are more air molecules available to produce more LNOx. Indeed, the laboratory measurements of Wang et al. [1998] show an increase of NO_x production with increasing pressure, all else being equal. Finally, LNOx production also depends on the current waveform associated with the lightning discharge. This is a more complicated comparison to make, as there are several discharge types even with a given flash type (ground or cloud). The peak current and current duration clearly are important parameters to consider.

Given the longer channel lengths and lower channel altitudes of ground flashes, and all the available NO_x production mechanisms available in Wang et al. [1998] and Cooray et al. [2009], including those production mechanisms related to the current waveform, the LNOM obtains the LNOx distributions (LND product) shown in Figure 5.5 (for the same 9 year period mentioned above). It is interesting to see that the average LNOx per ground flash is 604.3 moles, whereas it is only 36.4 moles for cloud flashes. Averaging the entire sample of flashes gives a value of 94.4 moles per flash; note that in the total sample of 404,197 flashes there are far more cloud flashes (364,031 or 90.1%) than there are ground flashes (40,166 or 9.9%).

It should also be noted that LNOM flash counts are not suitable for estimating the ratio of the number of cloud flashes to ground flashes, or so-called "Z ratio." For example, flashes are removed from all LNOM data products if the flash type cannot be confidently determined by the, non-exhaustive but efficient, analysis of the NLDN and LMA data.

One should also note that Table 5.1 shows updated values of P and P/N_A for the LNOM data analysis based on the 9 years of North Alabama data in the LNOM archive. Previously, the best values shown for LNOM data analyses given in Koshak et al., [2013] were based on just five summer months of analyses (i.e., August 2005, August 2006, August 2007, August 2008, and August 2009), or a total of 32,705 flashes. Of the 32,705 flashes, 4832 were ground flashes and 27,873 were cloud flashes. The average LNOx per ground flash was 484.15 moles, and the average for cloud flashes was 34.78 moles. So the average LNOx per flash was computed as [4832(484.15)+27873(34.78)]/32705 = 101.17 moles/flash. However, this (correct) result is susceptible to misinterpretation. Obviously, it is biased downward because the number of cloud flashes employed in the computation far outnumbers the number of ground flashes used. Hence, it is more meaningful to properly weight the relative frequencies of ground and cloud flashes. To do this, one can use the value of the mean Z ratio equal to 3 for the months of August that Koshak et al. [2013] found from the 4 year climatological Z-ratio dataset obtained by Boccippio et al. [2001]. The computation then becomes: [1(484.15)+3(34.78)]/4 = 147.12 moles/flash (for the month of August in North Alabama). As seen in Figure 5.5, the 9 year North Alabama data from the LNOM archive consists of a total of 404,197 flashes (40,166 ground flashes + 364,031 cloud flashes). Using the mean LNOx per ground and per cloud flash from Table 5.5, the mean is [40,166(604.28)+364,031(38.19)]/404,197 = 94.4 moles/flash as stated above. But again, it is more meaningful to use an estimate of the relative frequencies of ground and cloud flashes. Across all months and for the North Alabama region, the mean value of the Z-ratio is about 2 [Boccippio et al., 2001]. Therefore, a more meaningful value for the mean LNOx per flash is [1(604.28)+2(38.19)]/3 = 226.89 moles/flash which is the value shown in Table 5.1.

The LNOM archive continues to grow, and this trend is expected to continue especially with the proliferation of VHF networks. The LNOM database will likely expand by analyzing flashes detected by other VHF networks in the following areas: Oklahoma, West Texas, Houston, White Sands in New Mexico, Fort Collins (as part of the National Science Foundation (NSF) DC3 Experiment), Sao Paulo, Brazil (as part of the CHUVA Experiment), Dugway Proving Ground in Utah, Camp Blanding Florida, Kennedy Space Center Florida [both Lightning Detection And Ranging II (LDAR II), and a new lightning mapping array due to be installed], and potentially other regions. In the case of the Sao Paulo network, Vaisala's TLS200 measurements could be used as a substitute for NLDN data.

Overall, the frequency distributions of LNOx production, $\Phi(p_g)$ and $\Phi(p_c)$, derived from LNOM and shown in the two right-most panels of Figure 5.5 could be considered for replacing the two fixed educated guesses (P_g, P_c) for production currently employed within ModelE2 as discussed in section 5.4.1. That is, there is no longer a need to restrict the LNOx production parameterization to a single fixed "back-of-the-envelope" estimate (i.e., one estimate for ground flashes, and one estimate for cloud flashes). With the processing of detailed lightning observations by LNOM, the statistical frequency distributions, $\Phi(p_g)$ and $\Phi(p_c)$, of LNOx production from *actual* ground and cloud flashes is available. Specifically, instead of assigning to each ground flash the same fixed LNOx production value, one can randomly pick the LNOx production value from LNOM-derived distribution $\Phi(p_g)$. A similar comment holds for the cloud flashes. Because of the random sampling, this general approach also makes it possible to create more realistic simulations of the temporal evolution of the LNOx source within models, particularly in those models that are geared toward shorter-term forecasts (such as with CMAQ ozone predictions).

5.4.5 Future Evolution

Although the LNOM has made significant advances in combining theory, lab results, and flash-specific measurements to acquire optimal estimates of LNOx, it is recognized that it is still an imperfect tool.

First, a comprehensive list of LNOx production mechanisms is not available for LNOM to apply, and of those mechanisms identified in the scientific literature, there is still debate as to their relative importance. In particular, less is known about the discharge physics processes within cloud flashes, so it is possible that LNOM presently does not correctly parameterize LNOx from cloud flashes. For example, and as discussed above, there is evidence that cloud flashes might produce as much NO_x as ground flashes; i.e., the rocket-triggered lightning study of Rahman et al. [2007] indicated that the discharge processes associated with small, slower, steady currents produced substantial NO_x. Yet, the present cloud flash LNOx parameterizations employed by LNOM lead to relatively small values of cloud flash NO_x. It is too early to tell how such an issue will eventually be resolved, and debate on whether a typical cloud flash produces less, about the same, or even more NO_x than a typical ground flash continues. As such, the LNOM architecture is highly modular so that LNOx parameterizations for different discharge processes can be easily refined, or new parameterizations added via a "plug-and-play" methodology. As the LNOM matures along these lines, reprocessing of the LNOM input (NLDN and VHF) data archive will provide updated LNOM results for the lightning/chemistry community.

Second, estimating lightning channel length from LMA VHF sources is fundamentally difficult. Environmental radio frequency noise, source-strength degradation as a function of source range from the LMA network, and the lack of a consistent 1:1 relationship between the optical channel geometry and that defined by the channel VHF emission, all give rise to channel length estimation errors. Therefore, the LNOM software package is built in such a way that testing of alternative channel length modules is fairly easy.

The longer-term plans of the NASA Marshall Space Flight Center are to internally upgrade the main modules of LNOM, and reprocess the data archive with the latest LNOM version. Following the completion of this internal developmental phase (IDP), a broader community of expertise will be sought to further improve and test the LNOM. This community developmental phase (CDP) is anticipated to improve the accuracy and expand the applicability of the LNOM exponentially. This phase need not be limited to just software module improvements, but can also include ingestion of additional lightning/chemistry related measurements that "open the doors" for further improvements in estimating LNOx.

5.5 Benefits of Satellite Observations

In this section, some satellite-based observations of lightning, as well as satellite observations of the trace gas species affected by lightning, are discussed. In just the past ~50 years, advancements in space-borne measurements of lightning and its chemistry have provided a much better understanding of the global-scale spatio-temporal distribution of lightning and associated LNOx production. These global-scale features are difficult to obtain by conventional ground-based and aircraft observations alone.

5.5.1 Two Early Studies Employing Photometers

Space-based optical observations of lightning were conducted in the studies by Vorpahl et al. [1970] and Sparrow and Ney [1971] as part of the Orbiting Solar Observatory (OSO) series of satellites. The OSO Program was the name of a series of science satellites primarily for studying the Sun (i.e., to observe an 11-year sun spot cycle in UV and X-ray spectra), but also included important non-solar experiments. Eight satellites in the series were successfully launched by NASA between 1962-1975 using Delta rockets.

The study by Vorpahl et al. [1970] reported on night-time lightning activity from the OSO-2 satellite during the new Moon periods from February to October 1965. Three of four photometers sensitive to broad spectral bands and suitable for the detection of lightning within a 10^{o} field-of-view were employed. The minimum threshold of ~ 3 x 10^{5} photons cm^{-2} at the satellite was used, below which lightning could not be readily detected. The accuracy in determining the lightning source location was claimed to be better than ~ 3^{o} in latitude and longitude. Within the satellite observation limits of 35^{o} N to 35^{o} S, they determined that ten times as many lightning storms occur over land than over the ocean.

The investigation by Sparrow and Ney [1971] consisted of six photometers aboard the OSO-5 satellite. Four of the six photometers could be used to detect lightning, and the study reported on results from two of the four. The study confirmed Vorpahl's OSO-2 results that the distribution of night-time thunderstorms is heavily biased towards land areas rather than over ocean.

5.5.2 Space-Based Lightning Mappers

Since the early satellite photometer measurements mentioned above, additional optical observations of lightning have been made from the VELA and DMSP series of satellites, and from the space shuttle [Suszcynsky et al., 2001; Mackerras et al., 1998] and references therein.

However, an important advancement in better fixing the global annual lightning frequency, i.e., the variable *F* in equation (5.1), as well as vastly improving the understanding of the diurnal, seasonal and geographical variations in lightning and storm activity, was made possible by the advent of two satellite lightning mappers: the Optical Transient Detector (OTD; 1995-2000) and the Lightning Imaging Sensor (LIS; 1997-present). These instruments detect total (i.e. ground flash and cloud flash) lightning from low Earth orbit during both daytime and night [Christian et al., 1992, 1996, 1999, 2003]. Calibration and performance characteristics of the sensors are additionally given in Koshak et al., [2000] and Boccippio et al., [2000, 2002], respectively.

The OTD/LIS lightning mappers are based on Charge Coupled Device (CCD) imager technology that provides accurate geolocation with millisecond time resolution. OTD, a payload on the MicroLab-1 satellite (later renamed OV-1), had an average orbital altitude of about 740 km and a nadir pixel footprint of ~ 8x8 km^2. The LIS is aboard the Tropical Rainfall Measuring Mission (TRMM) satellite which had an average orbital altitude of about 350 km, but was later boosted to about 402.5 km in August 2001. The LIS nadir pixel footprint is ~ 4 x 4 km^2. Both the OTD and LIS employ a 128 x 128 pixel CCD array for geolocating lightning.

Since a flash typically last a few tenths of a second, and the OTD and LIS CCD frame times are ~ 2 ms, these instruments are ideal for examining the optical components of a flash. The nomenclature used to describe these components includes: *event*, *group*, and *flash* [Mach et al., 2007]. Basically, an optical event is one (instrument threshold-breaking) pixel illumination in one CCD frame time; hence, an event is the basic unit of OTD/LIS data. An optical group is any collection of adjacent events in one frame time; "adjacent" here means that the pixels touch either on a side or a corner. Finally, the clustering of groups into a flash is performed in Earth-based coordinates. Figure 5.6 provides a global lightning flash density distribution based on OTD/LIS data [Mach et al., 2007].

Although the optical event, group, and flash data provide useful insight into lightning physics, the 2 ms frame time resolution is not sufficient for time-resolving individual lightning optical pulse waveforms, which typically have a pulse width at half maximum of ~ 400 μs, but with variability depending on the lightning discharge type [Goodman et al., 1988]. By comparison, photodiode/photometer sensors typically have excellent temporal resolution (e.g., 10-100 μs), but poor spatial resolution.

In addition to OTD and LIS, a Fast on-Orbit Recording of Transient Events (FORTE) satellite carrying VHF broadband receivers and an Optical Lightning System (OLS) was launched in 1997 [Suszcynsky et al., 2000]. The OLS consists of two optical systems. The first was the Lightning Location System (LLS), a 128 x 128 pixel CCD array for geolocating lightning flashes within 10 km. The front-end optical and CCD assemblies are identical to LIS. The second component of the OLS is a fast (15 μs resolution) broadband (0.4 – 1.1 μm) photometer with an 80^o field of view. This (augmented) lightning mapper was a joint Los Alamos National Laboratory and Sandia National Laboratories satellite experiment designed primarily to address technology issues associated with treaty verification and the monitoring of nuclear tests from space [Suszcynsky et al., 2000]. Inter-comparisons between the VHF and OLS

datasets have been used in an attempt to discriminate flash type (ground flash or cloud flash) from space, and in identifying specific discharge processes (e.g. return stroke signatures).

Recently, plans have been made to place a spare LIS on the International Space Station (ISS) in approximately January 2016. The 56^{o} orbital inclination of the ISS will allow the ISS/LIS to capture more lightning (such as thunderstorms over the upper Midwest of the US) that is presently missed by the 35^{o} orbital inclination of TRMM/LIS.

The future Geostationary Lightning Mapper (GLM) recently described in Goodman et al. [2013] is expected to have a profound impact on our understanding of LNOx production. It will map the locations and time-of-occurrence of total lightning activity *continuously* day and night with near-uniform storm-scale spatial resolution and with a product refresh rate of under 20 s over the Americas and adjacent oceanic regions. The GLM is based on the two heritage low Earth orbiting lightning mappers OTD and LIS, and it is planned as a payload on the Geostationary Operational Environmental Satellite R-series (GOES-R) which is presently scheduled to launch in early 2016. Although the primary objective of GLM is for severe weather warning (e.g., abrupt increases or "jumps" in lightning activity provide warning lead time to tornadic storms) the enormous lightning dataset that will be obtained through continuous monitoring will offer unprecedented detail and lightning statistics from which optimal estimates of LNOx production can be made. Likewise, other countries are planning similar missions [the Geostationary Lightning Imager (GLI) on China's Fengyun-4 (FY4) satellite series, and Europe's Lightning Imager (LI) as part of the Meteosat Third Generation (MTG) satellite series].

5.5.3 Top-Down Constraints on LNOx

The global model fit method (section 5.2.3) for estimating the global annual LNOx production G originally employed airborne observations of NO_x [Levy et al., 1996]. But, the method can also be applied using satellite observations of trace gases. For example, Boersma et al. [2005] extended the work of Levy et al. [1996] by employing satellite measurements of tropospheric NO_2 columns from the Global Ozone Monitoring Instrument (GOME). Satellite observations of this type offer a powerful "top-down" constraint on LNOx production when used in conjunction with a mature chemical transport model (CTM).

Another example of employing satellite observations is described in Martin et al. [2007]. Measurements of trace-gases from three satellite platforms were employed to provide independent top-down constraints on the LNOx source. The space-based measurements included: tropospheric NO_2 columns from the Scanning Imaging Absorption Spectrometer for Atmospheric Chartography (SCIAMACHY) [Bovensmann et al., 1999], tropospheric O_3 columns from the Ozone Monitoring Instrument (OMI) [Levelt et al., 2006] and Microwave Limb Sounder (MLS) [Waters et al., 2006], and upper tropospheric HNO_3 from the Atmospheric Chemistry Experiment Fourier Transform Spectrometer (ACE-FTS) [Bernath et al., 2005]. The global CTM employed was the GEOS-Chem model [Bey et al., 2001]. It was used to identify the locations and time periods in which lightning would be expected to dominate the trace gas observations. The space-based measurements were then sampled at those locations and time periods. All three measurements exhibited a maximum in the tropical Atlantic and a minimum in the tropical Pacific; the overall pattern was driven by injection of lightning NO into the upper troposphere over the tropical continents, followed by photochemical production of NO_2, HNO_3, and O_3 during transport. Using the distribution of lightning NO_x emissions in GEOS-Chem, the study found that a global emission rate of 6±2 Tg(N) yr^{-1} from lightning in the model best

represents the satellite observations of tropospheric NO_2, O_3, and HNO_3. If one applies equation (5.1), with the Cecil et al. [2012] global flash rate of 46 flashes/sec, one obtains an estimate $P = G/(\gamma F)$ = 17.8 x 10^{25} molecules/flash = 295.08 moles/flash. The LNOM estimate of 227.49 moles/flash given in Table 5.1 is within 23% [= (227.49-295.08)/295.08] of this value.

There is more than one way to view the inter-play or optimization process between bottom-up and top-down constraints for purposes of constraining the estimate of LNOx production. Figure 5.7 provides one way of conceptualizing the process. The various model parameterizations in the CTM involving lightning typically include: the lightning thundercloud flash rate parameterization (RP), the flash energy parameterization (EP), the LNOx yield parameterization (YP), and possibly even a vertical LNOx profile parameterization (PP). Additionally, OTD/LIS data, ground-based lightning data, lab data, algorithms, and advanced models are used to improve these parameterization. In principle, the EP, YP, and PP can all be adjusted in an attempt to maintain consistency with archived LNOM results.

Unfortunately, standard convective parameterizations in global CTMs fail to reproduce observations from OTD/LIS. But, the study by Murray et al. [2012] introduced an optimal regional scaling algorithm for CTMs to fit the LNOx source to the satellite lightning data in a way that preserves the coupling to deep convective transport; the coarse regional scaling preserves sufficient statistics in the satellite data to constrain the interannual variability of lightning. Using GEOS Chem as a test bed, they obtained a value of $G = 6.0 \pm 0.5$ Tg(N) yr^{-1}.

Recently, the uncertainties associated with applying top-down constraints have been examined [Stavrakou et al., 2013]. The top-down constraint approach implicitly assumes that the relationship between the emission fluxes and the atmospheric abundances is reasonably well simulated by the CTM, so that the CTM and measurement data mismatch can be mostly attributed to the errors in the emission inventories. However, studies mentioned in Stavrakou et al. [2013] point to flaws in the current mechanisms implemented in CTMs that imply potentially large impacts on simulated NO_x concentrations, and hence on the top-down NO_x emission estimates.

5.5.4 Discriminating Flash Type from Space

Although the lightning mappers discussed in section 5.5.2 are designed to provide total lightning activity, these optical instruments do not directly provide flash type (ground flash or cloud flash) classification; i.e., they do not determine the flashes that strike the ground. This is understandable since the optically thick thundercloud obscures the view making it difficult to determine flash type. Early examinations of data from the OTD and LIS confirm this difficulty. At optical frequencies, the thundercloud multiply scatters the lightning source, resulting in a diffuse cloud top emission that prevents one from deciding whether or not the lightning channel below cloud top connects to ground. The following subsection highlights the importance of determining flash type information when estimating LNOx production, and the last three subsections provide some recent advances in the development of retrieval algorithms that can be used to help segregate ground flashes from cloud flashes.

5.5.4.1 Why Discriminate?

In order to accurately estimate LNOx production for purposes of regional air quality and global chemistry/climate models, one needs to know how many flashes occur, and what amount of NO_x each flash produces. In addition, modelers need to know when and where the flashes

occur and at what altitude; this information allows them to simulate the time-dependent horizontal and vertical distributions of the LNOx source within their model grid system.

Rather than attempting to specify the LNOx produced from each flash, modelers usually assign a single, typical value of NO_x production P_g to all ground flashes, and a single, typical value P_c to all cloud flashes. This is done because ground and cloud flashes involve fundamentally different discharge processes and occur at different mean altitudes, and hence there is a reasonable expectation that the two flash types produce different amounts of NO_x.

Thus, modelers typically employ LNOx production parameterizations that specifically require estimates of the values of P_g and P_c. This implicitly implies that some knowledge of the relative number of ground and cloud flashes is needed. Even if a modeler assumes that $P_g = P_c$, there would still be a desire to discriminate the flash type of flashes observed from space because cloud flashes deposit NO_x at higher altitudes than ground flashes. Differences in the vertical distribution of the LNOx source directly affect predictions of ozone in both regional air quality and global climate/chemistry models.

Cloud flashes usually outnumber ground flashes by a typical ratio of 3:1, and this ratio can be substantially larger, particularly in severe storms. So even if P_c is chosen smaller than P_g, it is still possible that cloud flashes could be the dominant NO_x source.

Previous studies have used vertical profiles from Pickering et al. [1998] that were determined for a P_c/P_g ratio of 0.1, based on the work of Price et al. [1997]. However, some studies suggest that the P_c/P_g ratio might be closer to, or even above, unity [Gallardo and Cooray, 1996; DeCaria et al., 2000; Zhang et al., 2003; Fehr et al., 2004]; see Ott et al. [2010] for additional summary comments on the size of this ratio.

Presently however, the detailed analyses of the LNOM show that P_g is substantially larger than P_c [Koshak et al., 2013, Koshak and Peterson, 2011]. The difference is primarily attributable to differences in channel length, channel altitude, current magnitude, the number of strokes in a flash, and types of discharge-dependent NO_x production mechanisms present. In fact, because of the variable nature of lightning and thunderstorms, LNO_x production can substantially vary from one set of ground flashes to another, or from one set of cloud flashes to another. But, since less empirical data exists on cloud flashes overall, it is acknowledged that the parameterization of NO_x-production mechanisms within cloud flashes could be lacking and that future improvements to all LNOx parameterizations within the LNOM could tighten, or even close, the gap between the two flash types.

In any case, since the probability that P_g is *identically* equal to P_c is small, and since cloud flashes deposit more NO_x at higher altitudes than ground flashes, the best estimate of the overall LNOx source is obtained when one can segregate in some way the ground flashes from the cloud flashes. The next three subsections briefly summarize some methods for performing this segregation when satellite-based lightning mapper observations are employed.

5.5.4.2 The Mean Method

As mentioned previously, space-based optical observations of lightning normally cannot directly detect the discharge channel since it is typically obscured by the cloud. However, the spatio-temporal pattern of the diffuse lightning cloud top optical emission itself provides key information about whether or not the channel connects to ground. For example, by comparing OTD and NLDN data, Koshak [2010] showed that the mean Maximum Group Area (MGA) for ground flashes was appreciably larger than the mean MGA for cloud flashes, so that, for satellite

lightning mappers, MGA is a fundamental variable for discriminating ground flashes from cloud flashes. Here, a flash is composed of one or more optical groups, and the group of largest area is the MGA. It was hypothesized by Koshak [2010] that the return stroke, along with any accompanying simultaneous discharges, produces a relatively large optical group within the flash, so that a statistically large MGA is useful as a type of "return stroke detector."

The follow-on study by Koshak and Solakiewicz [2011] introduced a first attempt to retrieve the *ground flash fraction* based on the MGA variable suggested by Koshak [2010]. That is, given a set of N flashes observed by a satellite lightning mapper, the algorithm would estimate the fraction $\alpha = N_g/N$ of the flashes that strike the ground, where N_g is the number of ground flashes. The value of N must be large, typically 5000. Denoting x for the value of MGA and applying some straight-forward algebra, Koshak and Solakiewicz [2011] established a mathematical relationship between the mean MGA values and the ground flash fraction given by

$$\overline{x} = \alpha \overline{x}_g + (1-\alpha)\overline{x}_c \quad , \tag{5.7}$$

where $\overline{x}, \overline{x}_g$, and $\overline{x}_c$ are the mean MGA for all N flashes, for all N_g ground flashes, and for all $N_c = N - N_g$ cloud flashes, respectively. This equation is easily solved for α in terms of $\overline{x}, \overline{x}_g$, and $\overline{x}_c$. The value of $\overline{x}$ is computed directly from the N lightning mapper-observed values of MGA, and the values of $\overline{x}_g$ and $\overline{x}_c$ were estimated from the conterminus United States (CONUS) by comparing NLDN and OTD observations. Thus, retrieval errors obtained from this simple method are expected to increase when other geographical regions and seasons are considered.

5.5.4.3 The Mixed Exponential Distribution Method

A more sophisticated retrieval algorithm was introduced in Koshak [2011]. Rather than estimating the values of $\overline{x}_g$ and $\overline{x}_c$ with fixed CONUS means as was done in the mean method described above, this algorithm modeled the ground and cloud flash MGA density functions with distinct models. Each model had an exponential form after the low-ends of the ground and cloud flash MGA distributions were appropriately modified (i.e. shifted by the instrument nadir pixel footprint). By superpositioning these two exponential density function models, a single mixed exponential distribution model was obtained that could be used to described the distribution of measured MGAs. The mixed exponential distribution model had 3 parameters (α, μ_g, μ_c), where the last two parameters are the population means of the ground and cloud flash MGA distributions, respectively. The specific form of the mixed exponential distribution model is

$$p(y) = \frac{\alpha}{\mu_g} e^{-y/\mu_g} + \frac{(1-\alpha)}{\mu_c} e^{-y/\mu_c} \quad , \tag{5.8}$$

where y is the shifted MGA, and $p(y)$ is its associated density function. The values of these 3 parameters were retrieved from the MGA observations using a formal Bayesian inversion process and the maximum a posteriori (MAP) solution (see Koshak [2011] for additional details).

5.5.4.4 The Analytic Perturbation Method

Note that the mixed exponential distribution model discussed above is a *fixed* model and one attempts to find the optimum parameters of that fixed model. However, one can still argue that a different geographical region and/or season might have ground and cloud flash MGA population distributions that deviate too much from the fixed mathematical model employed. In addition, both the mean method and mixed exponential distribution method provide no way for flash typing specific flashes.

These limitations have motivated a very recent study by Koshak and Solakiewicz [2013]. They introduce a *model-independent* method for retrieving the ground flash fraction; the method also subsequently determines the flash type of each of the N flashes. Once again, the value of N must be large, typically 5000 (although reasonably small solution retrieval errors are obtained for values of N as low as 2000). The model-independent approach is called the Analytic Perturbation Method (APM).

The idea behind the APM is to avoid making any assumptions about how the MGAs are distributed in a particular geographical region for a particular period of time (e.g., season); the region and period are collectively referred to as the "target." To accomplish this, one carries out an instrument "burn-in" phase wherein the lightning mapper samples (typically thousands) of lighting in the target of interest. Using independent ground flash observations (e.g., NLDN, or GLD360 data) one can flash-type the sampled flashes observed by the lightning mapper, and therefore estimate the true ground and cloud flash MGA density functions. These "climate" density function estimates are then used as baselines or starting points in any actual subsequent retrieval.

In the subsequent operational retrieval, the lightning mapper makes an observation of $N \sim$ 5000 flashes in the target of interest. Next, the mathematical theory of the APM provides a way to perturb away from the climate baselines in order to retrieve, for the set of N observed flashes, the ground and cloud flash MGA density functions, the ground flash fraction, and the flash type of each flash. The APM solution for the retrieved ground flash fraction α_r and the retrieved ground and cloud flash MGA density functions, described by the vectors ($\mathbf{g}_r$, $\mathbf{c}_r$), is given by (see derivation given in Koshak and Solakiewicz [2013]):

$$\begin{aligned} \alpha_r &= \frac{(\mathbf{m}-\mathbf{b})^T(\mathbf{a}-\mathbf{b})}{(\mathbf{a}-\mathbf{b})^2} \\ \mathbf{g}_r &= \mathbf{m} + (1-\alpha_r)(\mathbf{a}-\mathbf{b}) \\ \mathbf{c}_r &= \mathbf{m} - \alpha_r(\mathbf{a}-\mathbf{b}) \ . \end{aligned} \tag{5.9}$$

Here, the climate ground and cloud flash MGA density functions are described by the vectors (**a**, **b**). The frequency distribution of the observed MGA values can be described by a vector **M**; dividing this vector by the sample size N gives the vector **m**. So **m** is a measured quantity provided by the lightning mapper. Mathematically, **m** is a vector that describes the MGA mixture density; i.e., $\mathbf{m} = \alpha\mathbf{g} + (1-\alpha)\mathbf{c}$ where (**g**, **c**) are vectors that describe the true ground and cloud flash MGA density functions. The APM solutions in equation (5.9) provide the retrieval estimates to each term on the right hand side of this expression of **m**.

Using the results in equation (5.9), Koshak and Solakiewicz [2013] obtained the probability, $P_{gr}(x)$, that a flash, having an MGA value equal to x, is a ground flash. The expression they derived is given by

$$P_{gr}(x) = \frac{\alpha_r g_r(x)}{\alpha_r g_r(x) + (1-\alpha_r) c_r(x)} \quad . \tag{5.10}$$

The values on the right hand side of equation (5.10) are given in equation (5.9) where the density functions $g_r(x)$ and $c_r(x)$ are described by the vectors $\mathbf{g}_r$ and $\mathbf{c}_r$, respectively. The flash typing approach is straightforward; i.e., $P_{gr}(x) > 0.5 \Rightarrow$ ground flash, and $P_{gr}(x) \leq 0.5 \Rightarrow$ cloud flash. Koshak and Solakiewicz [2013] performed detailed simulations and found that the APM performed quite well; the mean ground flash fraction retrieval errors were below 0.04 across the full range 0-1, and the fraction of flashes accurately flash typed averaged better than 78%.

If it is not feasible or possible to conduct a burn-in process for a particular target, call it target A, it is possible to apply to target A the burn-in results (i.e. climate vectors) from a different target (target B). However, retrieval errors will be large if the thunderstorm and lightning characteristics of target A differ from those of target B.

Overall, the basic idea is to provide the lightning mapper sufficient "training" via the burn-in approach so that the lightning mapper can then run autonomously for a wide range of targets, including possibly those targets that may have no, or inadequate, independent lightning flash type validation measurements available.

The ideal future application of the APM is to apply it to the global OTD/LIS climatology in order to partition the lightning climatology into separate ground and cloud flash climatologies. Optimal estimates of the NO_x produced per ground and per cloud flash, possibly by future improved versions of the LNOM containing updated parameterizations for cloud flashes, could then be applied to these climatologies to recalculate the global LNOx production, G. Of course, this estimate could be updated once again in the same manner as future GLM, GLI, ISS/LIS, and LI data become available.

5.6 References

Aghedo, A. M., K. W. Bowman, H. M. Worden, S. S. Kulawik, D. T. Shindell, J. F. Lamarque, G. Faluvegi, M. Parrington, D. B. A. Jones, and S. Rast, The vertical distribution of ozone instantaneous radiative forcing from satellite and chemistry climate models, *J. Geophys. Res*., **116**, D01305, doi:10.1029/2010JD014243, 2011.

Albrecht, R. I., C. A. Morales, and M. A. F. Silva Dias, Electrification of precipitating systems over the Amazon: Physical processes of thunderstorm development. *J. Geophys. Res.*, **116**, D08209,10.1029/2010JD014756, 2011.

Baker, M. B., Christian, H. J., Latham, J., A computational study of the relationships linking lightning frequency and other thundercloud parameters, *Quart. J. Roy. Met. Soc.*, **121**, 1525-1548, 1995.

Baker, M. B., Blyth, A. M., Christian, H. J., Latham, J., Miller K. L., Gadian, A. M., Relationships between lightning activity and various thundercloud parameters: satellite and modeling studies, *Atmos. Res.*, **51**, 221-236, 1999.

Beirle, S., U. Platt, M. Wenig, and T. Wagner, NO_x production by lightning estimated with GOME, *Adv. Space Res.*, **34**, 793-797, 2004.

Beirle, S., N. Spichtinger, A. Stohl, et al., Estimating the NO_x produced by lightning from GOME and NLDN data: a case study in the Gulf of Mexico, *Atmos. Chem. Phys.,* **6**, 1075-1089, http://www.atmos-chem-phys.net/6/1075/2006/, 2006.

Beirle, S., H. Huntrieser, and T. Wagner, Direct satellite observation of lightning-produced NO_x, *Atmos. Chem. Phys.*, **10**, 10965-10986, 2010.

Bernath, P. F., C. T. McElroy, M. C. Abrams, et al., Atmospheric Chemistry Experiment (ACE): mission overview, *Geophys. Res. Lett.*, **32**, L15S01, doi:10.1029/2005GL022386, 2005.

Betz, H.-D., K. Schmidt, W. P. Oettinger, and M. Wirz, Lightning detection with 3D-discrimination of intracloud and cloud-to-ground discharges, *Geophys. Res. Lett.*, **31**, L11108, doi:10.1029/2004GL019821, 2004.

Betz, H.-D., K. Schmidt, B. Fuchs, W. P. Oettinger, and H. Höller, Cloud lightning: detection and utilization for total lightning measured in the VLF/LF regime, *J. Lightning Res.*, **2**, 1–17, 2007.

Bey, I., D. J. Jacob, R. M. Yantosca, J. A. Logan, B. D. Field, A. M. Fiore, Q. Li, H. Y. Liu, L. J. Mickley, M. G. Schultz, Global modeling of tropospheric chemistry with assimilated meteorology: Model description and evaluation, *J. Gephys. Res.*, **106**, 23073-23096, 2001.

Bhetanabhotla, M. N., B. A. Crowell, A. Coucouvinos, R. D. Hill, and R. G. Rinker, Simulation of trace species production by lightning and corona discharge in moist air, *Atmos. Environ.*, **19**, 1391-1397, 1985.

Biazar, A. P., and R. T. McNider, Regional estimates of lightning production of nitrogen oxides, *J. Geophys. Res.*, **100**, D11, 22861-22874, 1995.

Boccippio D. J., W. J. Koshak, R. J. Blakeslee, K. Driscoll, D. Mach, D. E. Buechler, W. Boeck, H. J. Christian, S. J. Goodman, The Optical Transient Detector (OTD): instrument characteristics and cross-sensor validation, *J. Atmos. Oceanic Technol.*, **17**, 441-458, 2000.

Boccippio, D. J., K. L. Cummins, H. J. Christian, and S. J. Goodman, Combined satellite and surface-based estimation of the intracloud:cloud-to-ground lightning ratio over the continental United States, *Mon. Weather Rev.*, **129**, 108-122, 2001.

Boccippio, D. J., W. J. Koshak, R. J. Blakeslee, Performance assessment of the Optical Transient Detector and Lightning Imaging Sensor. Part I: predicted diurnal variability, *J. Atmos. Oceanic Technol.*, **19**, 1318-1332, 2002.

Boccippio, D. J., Lightning scaling relations revisted, *J. Atmos. Sci.*, **59**, 1086-1104, 2002.

Boersma, K. F., H. J. Eskes, E. W. Meijer, and H. Kelder, Estimates of lightning NO_x production from GOME satellite observations, *Am. Chem. Phys.*, **5**, 2311-2331, 2005.

Borucki, W. J. and W. L. Chameides, Lightning: estimates of the rates of energy dissipation and nitrogen fixation, *Rev. Geophys. Space Phys.*, **22**, 363-372, 1984.

Bovensmann, H., J. P. Burrows, M. Buchwitz, J. Frerick, V. V. Rozanov, K. V. Chance, and A. P. H. Goede, SCIAMACHY: mission objectives and measurement modes, *J. Atmos. Sci.*, **56**(2), 127-150, 1999.

Bradshaw, J., D. Davis, G. Grodzinsky, S. Smyth, R. Newell, S. Sandholm, and S. Liu, Observed distributions of nitrogen oxides in the remote free troposphere from the NASA Global Tropospheric Experiment programs, *Rev. Geophys.*, **38**, 61-116, doi:10.1029/1999RG900015, 2000.

Brooks, C. E. P., The distribution of thunderstorms over the globe, *Geophys Mem.*, **3** (4), 147-164, 1925.

Bucsela, E. J., K. E. Pickering, T. L. Huntemann, R. C. Cohen, A. Perring, J. F. Gleason, R. J. Blakeslee, R. I. Albrecht, R. Holzworth, J. P. Cipriani, D. Vargas-Navarro, I. Mora-Segura, A. Pacheco-Hernandez, and S. Laporte-Molina, Lightning-generated NOx seen by the Ozone Monitoring Instrument during NASA's Tropical Composition, Cloud and Climate Coupling Experiment (TC4), *J. Geophys. Res.*, **115**, D00J10, doi:10.1029/2009JD013118, 2010.

Carey, L. D., and S. A. Rutledge, Electrical and multiparameter radar observations of a severe hailstorm, *J. Geophys. Res.*, **103**, 13979-14000, 1998.

Casper, P. W., and R. B. Bent, Results from the LPATS USA national lightning detection and tracking system for the 1991 lightning season, *Proc. 21st Int. Conf. Lightning Protection*, Berlin, Germany, pp. 339-342, Sept., 1992.

Cecil, D. J., D. E. Buechler, and R. J. Blakeslee, Gridded lightning climatology from TRMM-LIS and OTD: dataset description, *Atmo. Res.*, doi:10.1016/j.atmosres.2012.06.028, 2012.

Chameides, W. L., and J. C. G. Walker, A photochemical theory of tropospheric ozone, *J. Geophys. Res.*, **78**, 8751-8760, 1973.

Chameides, W. L., D. H. Stedman, R. R. Dickerson, D. W. Rusch, and R. J. Cicerone, NO_x production in lightning, *J. Atmo. Sci.*, **34**, 143-149, 1977.

Chameides, W. L., Effect of variable energy input on nitrogen fixation in instantaneous linear discharges, *Nature*, **277**, 123-125, 1979.

Chameides, W. L., The role of lightning in the chemistry of the atmosphere. In *The Earth's Electrical Environment*, Chapter 6, National Academy Press, Washington, D. C., ISBN 0-309-03680-1, 1986.

Chameides, W. L., D. D. Davis, J. Bradshaw, M. Rodgers, S. Sandholm, and D. B. Bai, An estimate of the NO_x production rate in electrified clouds based on NO observations from the GTE/CITE 1 fall 1983 field operation, *J. Geophys. Res.*, **92**, 2153-2156, 1987.

Christian, J. J., R. J. Blakeslee, and S. J. Goodman, Lightning Imaging Sensor for the Earth Observing System, in *Tech. Rep. NASA TM-4350*, NASA, Washington, D. C., 1992.

Christian, J. J., K. T. Driscoll, S. J. Goodman, R. J. Blakeslee, D. M. Mach, and D. E. Buechler, The Optical Transient Detector (OTD), in *Proc. 10th Int. Conf. on Atmospheric Electricity*, 368-371, ICAE, Osaka, Japan, 1996.

Christian, H. J., R. J. Blakeslee, S. J. Goodman, D. M. Mach, M. F. Stewart, D. E. Buechler, W. J. Koshak, J. M. Hall, W. L. Boeck, K. T. Driscoll, and D. J. Boccippio, The Lightning Imaging Sensor, in *Proc. 11th Int. Conf. on Atmospheric Electricity*, 746-749, ICAE, Guntersville, AL, 1999.

Christian, H. J., R. J. Blakeslee, D. J. Boccippio, W. L. Boeck, D. E. Buechler, K. T. Driscoll, S. J. Goodman, J. M. Hall, W. J. Koshak, D. M. Mach, M. F. Stewart, Global frequency and distribution of lightning as observed from space by the Optical Transient Detector, *J. Geophys. Res.*, **108**, No. D1, doi:10.1029/2002JD002347, 2003.

Cook, D. R., Y. P. Liaw, D. L. Sisterson, and N. L. Miller, Production of nitrogen oxides by a large spark generator, *J. Geophys. Res.*, **105**, 7103-7110, doi:10.1029/1999JD901138, 2000.

Cooray, V., M. Rahman, V. Rakov, On the NO_x production by laboratory electrical discharges and lightning, *J. of Atmos. & Solar-Terres. Phys.*, **71**, 1877-1889, 2009.

Crutzen, P. J., The influence of nitrogen oxides on the atmospheric ozone content, *Quart. J. Roy. Meteor. Soc.*, **96**, 320-327, 1970.

Crutzen, P. J., A discussion of the chemistry of some minor constituents in the stratosphere and troposphere, *Pure Appl. Geophys.*, **106**, 1385-1399, 1973.

Crutzen, P. J., The role of NO and NO_2 in the chemistry of the troposphere and stratosphere, *Ann. Rev. Earth Planet. Sci.*, **7**, 443-472, 1979.

Cummins, K. L., J. A. Cramer, C. J. Biagi, E. P. Krider, J. Jerauld, M. A. Uman, V. A. Rakov, The US National Lightning Detection Network: post-upgrade status, *Second Conference on Meteorological Applications of Lightning Data*, Am. Meteorol. Soc., Atlanta, Ga., 29 January to 2 February, 2006.

Cummins, K. L. and M. J. Murphy, An overview of lightning locating systems: history, techniques, and data uses, with an in-depth look at the U. S. NLDN, *IEEE Trans. on Electromag. Comp.*, **51**, No. 3, 499-518, 2009.

Dawson, G. A., Nitrogen fixation by lightning, *J. Atmos. Sci.*, **37**, 174-178, 1980.

DeCaria, A. J., K. E. Pickering, G. L. Stenchikov, J. R. Scala, J. L. Stith, J. E. Dye, B. A. Ridley, and P. Laroche, A cloud-scale model study of lightning-generated NO_x in an individual thunderstorm during STERAO-A, *J. Geophys. Res.*, **105**, 11601-11616, 2000.

DeCaria, A. J., K. E. Pickering, G. L. Stenchikov, and L. E. Ott, Lightning-generated NO_x and its impact on tropospheric ozone production: a three-dimensional modeling study of a Stratosphere-Troposphere Experiment: Radiation, Aerosols, and Ozone (STERAO-A) thunderstorm, *J. Geophys. Res.*, **110**, D14303, doi:10.1029/2004JD005556, 2005.

Depasse, P., Statistics on artificially triggered lightning, *J. Geophys. Res.*, **99**, D9, 18515-18522, 1994.

Drapcho, D. L., D. Sisterson, and R. Kumar, Nitrogen fixation by lightning activity in a thunderstorm, *Atmos. Environ.*, **17**, 729-734, 1983.

Dye, J. E., B. A. Ridley, W. Skamarock, et al.: An overview of the Stratospheric-Tropospheric Experiment: Radiation, Aerosols, and Ozone (STERAO)-Deep convection experiment with results for the July 10, 1996 storm, *J. Geophys. Res.*, **105**, 10023-10045, 2000.

Edwards, D. P., J. F. Lamarque, J. L. Attie, L. K. Emmons, A. Richter, J. P. Cammas, J. C. Gille, G. L. Francis, M. N. Deeter, J. Warner, D. C. Ziskin, L. V. Lyjak, J. R. Drummond, and J. P. Burrows, Tropospheric ozone over the tropical Atlantic: a satellite perspective, *J. Geophys. Res.,* **108**, No. D8, 4237-4257, 2003.

Fehr, T., H. Holler, and H. Huntrieser, Model study on production and transport of lightning-produced NO_x in an EULINOX supercell storm, *J. Geophys. Res.*, **109**, D09102, doi:10.1029/2003JD003935, 2004.

Fieux, R., C. Gary, P. Hubert, Artificially triggered lightning above land, *Nature*, **257**, 212-214, 1975.

Franzblau, E. and C. J. Popp, Nitrogen oxides produced from lightning, *J. Geophys. Res.*, **94**, 11089-11104, doi:10.1029/89JD00694, 1989.

Fraser, A., F. Goutail, C. A. McLinden, S. M. L. Melo, and K. Strong, Lightning-produced NO_2 observed by two ground-based UV-visible spectrometers at Vanscoy, Saskatchewan in August 2004, *Atmos. Chem. Phys.*, **7**, 1683-1692, http://www.atmos-chem-phys.net/7/1683/2007/, 2007.

Gallardo, L., and V. Cooray, Could cloud-to-cloud discharges be as effective as cloud-to-ground discharges in producing NOx?, *Tellus*, **48B**, 641–651, 1996.

Goldenbaum, G. C. and R. R. Dickerson, Nitric oxide production by lightning discharges, *J. Geophys. Res.*, **98**, 18333-18338, 1993.

Goodman, S. J., H. J. Christian, W. D. Rust, A comparison of the optical pulse characteristics of intracloud and cloud-to-ground lightning as observed above clouds, *J. Appl. Meteorol.*, **27**, 1369-1381, 1988.

Goodman, S. J., R. J. Blakeslee, W. J. Koshak, D. M. Mach, J. C. Bailey, D. E. Buechler, L. D. Carey, C. D. Schultz, M. Bateman, E. W. McCaul, G. Stano, The GOES-R Geostationary Lightning Mapper (GLM), *Atmos. Res.*, **125-126**, 34-49, 2013.

Grewe, V., C. Reithmeier, and D. Shindell, Dynamic-chemical coupling of the upper troposphere and lower stratosphere region, *Chemosphere*, **47/8**, 55-65, 2002.

Grewe, V., D.T. Shindell, and V. Eyring, The impact of horizontal transport on the chemical composition in the tropopause region: Lightning NO_x and streamers, *Adv. Space Res.*, **33**, 1058-1061, doi:10.1016/S0273-1177(03)00589-1, 2004.

Hameed, S., O. G. Paidoussis, and R. W. Stewart, Implication of natural sources for the latitudinal gradients of NO_y in the unpolluted troposphere, *Geophys. Res. Lett.*, **8**, 591-594, 1981.

Heckman, S. J., Williams, E. R., Boldi, R., Total global lightning inferred from Schumann resonance measurements, *J. Geophys. Res.*, **103**, D24, 31775-31779, 1998.

Hidalgo, H. and P. J. Crutzen, The tropospheric and stratospheric composition perturbed by NO_x emissions of high-altitude aircraft, *J. Geophys. Res.*, **82**, 5833-5866, 1977.

Hill, R. D., R. G. Rinker, and H. D. Wilson, Atmospheric nitrogen fixation by lightning, *J. Atmos. Sci.*, **37**, 179-192, 1980.

Höller, H., U. Finke, H. Huntrieser, M. Hagen, and C. Feigl, Lightning-produced NO_x (LINOX): experimatal design and case study results, *J. Geophys. Res.*, **104**, 13911-13922, doi:10.1029/1999JD900019, 1999.

Höller, H., and U. Schumann (Eds.), EULINOX-The European Lightning Nitrogen Oxides Project, *Rep. DLR-FB 2000-28,* 240 pp., Deutsche Luftund Raumfahrt Oberpfaffenhofen, Wessling, Germany, 2000.

Höller, H., H.-D. Betz, K. Schmidt, R. V. Calheiros, P. May, E. Houngninou, and G. Scialom, Lightning characteristics observed by a VLF/LF lightning detection network (LINET) in Brazil, Australia, Africa and Germany, *Atmos. Chem. Phys.*, **9**, 7795-7824, 2009.

Huff, F. A., Changnon Jr., S. A., Inadvertent precipitation modification by urban areas, *Preprints in 3rd Conf. on Weather Modification*, AMS, Boston, MA, pp. 73-78, 1972.

Huntrieser, H., H. Schlager, C. Feigl, and H. Höller, Transport and production of NO_x in electrified thunderstorms: Survey of previous studies and new observations at midlatitudes, *J. Geophys. Res.*, **103**, 28247-28264, 1998.

Huntrieser, H. H., C. Feigl, H. Schlager, et al., Airborne measurements of NO_x, tracer species, and small particles during the European Lightning Nitrogen Oxides Experiment, *J. Geophys. Res.*, **107**, 4113, doi:10.1029/2000JD000209, 2002.

Huntrieser, H., H. Schlager, A. Roiger, U. Schumann, H. Höller, C. Kurz, D. Brunner, C. Schwierz, A. Richter, and A. Stohl, Lightning-produced NO_x over Brazil during TROCCINOX: airborne measurements in tropical and subtropical thunderstorms and the importance of mesoscale convective systems, *Atmos. Chem. Phys.*, **7**, 2987-3013, http://www.atmos-chem-phys.net/7/2987/2007/, 2007.

Huntrieser, H., U. Schumann, H. Schlager, H. Höller, A. Giez, H.-D. Betz, D. Brunner, C. Forster, O. Pinto Jr., and R. Calheiros, Lightning activity in Brazilian thunderstorms during TROCCINOX: implications for NO_x production, *Atmos. Chem. Phys.*, **8**, 921-953, 2008.

Huntrieser, H., H. Schlager, M. Lichtenstern, P. Stock, T. Hamburger, H. Höller, K. Schmidt, H.-D. Betz, A. Ulanovsky, and F. Ravegnani, Mesoscale convective systems observed during AMMA and their impact on the NOx and O3 budget over West Africa, *Atmos. Chem. Phys*., **11**, 2503-2536, doi:10.5194/acp-11-2503-2011, 2011.

Hutchinson, G. E., The biogeochemistry of the terrestrial atmosphere. In *The Earth as a Planet*, ed. G. P. Kuiper, University of Chicago Press, Chicago, 1954.

IPCC Second Assessment Report: Climate Change 1995, A report of the Intergovernmental Panel on Climate Change (IPCC).

Jadhav, D. B., A. L. Londhe, S. Bose, Observations of NO_2 and O_3 during thunderstorm activity using visible spectroscopy, *Adv. Atmos. Sci.*, **13**, 359-374, 1996.

Jourdain, L., S. S. Kulawik, H. M. Worden, K. E. Pickering, J. Worden, and A. M. Thompson, Lightning NO_x emissions over the USA constrained by TES ozone observations and the GEOS-Chem model, *Atmos. Chem. Phys.*, **10**, 107-119, 2010.

Koike, M., Y. Kondo, K. Kita, et al., Measurements of reactive nitrogen produced by tropical thunderstorms during BIBLE-C, *J. Geophys. Res.*, **112**, D18304, doi:10.1029/2006JD008193, 2007.

Koshak, W. J., M. F. Stewart, H. J. Christian, J. W. Bergstrom, J. M. Hall, and R. J. Solakiewicz, Laboratory Calibration of the Optical Transient Detector and the Lightning Imaging Sensor, *J. Atmos. Oceanic Technol.*, **17**, 905-915, 2000.

Koshak, W. J., R. J. Solakiewicz, R. J. Blakeslee, S. J. Goodman, , H. J. Christian, J. M. Hall, J. C. Bailey, E. P. Krider, M. G. Bateman, D. J. Boccippio, D. M. Mach, E. W. McCaul, M. F. Stewart, D. E. Buechler, W. A. Petersen, D. J. Cecil, North Alabama Lightning Mapping Array (LMA): VHF source retrieval algorithm and error analyses, *J. Atmos. Oceanic Technol*., **21**, 543-558, 2004.

Koshak, W. J., M. N. Khan, A. P. Biazar, M. Newchurch, R. T. McNider, A NASA model for improving the lightning NO_x emission inventory for CMAQ, *Joint Session: 4th Conference on the Meteorological Applications of Lightning Data and and the 11th Conference on Atmospheric Chemistry; 89th Annual AMS Conference*, Phoenix, AZ, January 11-15, 2009.

Koshak, W. J., H. S. Peterson, E. W. McCaul, A. Biazar, Estimates of the lightning NO_x profile in the vicinity of the North Alabama Lightning Mapping Array, *International Conference on Lightning Detection*, Orlando, FL, April 19-21, 2010.

Koshak, W. J., Optical characteristics of OTD flashes and the implications for flash-type discrimination, *J. Atmos. Oceanic Technol*., **27**, 1822-1838, 2010.

Koshak, W. J., and R. J. Solakiewicz, Retrieving the fraction of ground flashes from satellite lightning imager data using CONUS-based optical statistics, *J. Atmos. Oceanic Technol*., **28**, 459-473, 2011.

Koshak, W. J., A mixed exponential distribution model for retrieving ground flash fraction from satellite lightning imager data, *J. Atmos. Oceanic Technol*., **28**, 475-492, 2011.

Koshak, W., H. Peterson, M. Khan, A. Biazar, L. Wang, The NASA Lightning Nitrogen Oxides Model (LNOM): Application to Air Quality Modeling, *XIV International Conference on Atmospheric Electricity*, Rio de Janeiro, Brazil, August 8-12, 2011.

Koshak, W., and H. Peterson, A summary of the NASA Lightning Nitrogen Oxides Model (LNOM) and recent results, *10th Annual Community Modeling and Analysis System (CMAS) Conference*, Chapel Hill, NC, October 24-26, 2011.

Koshak, W. J., H. S. Peterson, A. P. Biazar, M. Khan, and L. Wang, The NASA Lightning Oxides Model (LNOM): application to air quality modeling, *Atmos. Res.*, http://dx.doi.org/10.1016/j.atmosres.2012.12.015, 2013.

Koshak, W. J. and R. J. Solakiewicz, A method for retrieving the ground flash fraction and flash type from satellite lightning mapper observations, submitted to *J. Atmos. Oceanic Technol*., 2013.

Kotaki, M., I. Kuriki, C. Katoh, and H. Sugiuchi, Global distribution of thunderstorm activity observed with ISS-b, *J. Radio Res. Lab. Jpn.*, **28**, 49-71, 1981.

Kowalczyk, M. and E. Bauer, Lightning as a source of NO_x in the troposphere, Tech. Rep. FAA-EE-82-4, 76 pp., *Inst. For Def. Anal.*, Alexandria, Virginia, 1982.

Kumar, P. P., G. K. Manohar, and S. S. Kandalgaonkar, Global distribution of nitric oxide produced by lightning and its seasonal variation, *J. Geophys. Res.*, **100**, 11203-11208, 1995.

Kunkel, K. E., Sea surface temperature forcing of the upward trend in US extreme precipitation, *J. Geophys. Res.*, **108**, D1, 4020, doi:10.1029/2002JD002404, 2003.

Labrador, L. J., R. von Kuhlmann, M. G. Lawrence, The effects of lightning-produced NO_x and its vertical distribution on atmospheric chemistry: sensitivity simulations with MATCH-MPIC, *Atmos. Chem. Phys. Discuss*., **4**, 6239-6281, 2004.

Langford, A. O., R. W. Portmann, J. S. Daniel, H. L. Miller, and S. Solomon, Spectroscopic measurements of NO_2 in a Colorado thunderstorm: determination of the mean production by cloud-to-ground lightning flashes, *J. Geophys. Res.*, **109**, D11304, doi:10.1029/2003JD004158, 2004.

Lawrence, M. G., W. L. Chameides, P. S. Kasibhatla, H. Levy, II, and W. Moxim, Lightning and atmospheric chemistry: The rate of atmospheric NO production, in *Handbook of Atmospheric Electrodynamics*, vol. 1, edited by H. Volland, pp. 189-202, CRC Press, Boca Raton, Florida, 1995.

Levelt, P. F., G. H. J. van den Oord, M. R. Dobber, A. Mslkki, H. Visser, J. Vries, P. Stammes, J. O. V. Lundell, and H. Saari, The Ozone Monitoring Instrument, *IEEE Trans. Geosci. Remote Sens.*, **44**, 1093-1101, doi:10.1109/TGRS.2006.872333, 2006.

Levine, J. S., Simultaneous measurements of NO_x, NO, and O_3 production in a laboratory discharge: atmospheric implications, *Geophys. Res. Lett.*, **8**, 357-360, 1981.

Levy, H., W. J. Moxim, and P. S. Kasibhatla, A global three-dimensional time-dependent lightning source of tropospheric NO_x, *J. Geophys. Res.*, **101**, 22911-22922, 1996.

Liaw, Y. P., D. L. Sisterson, and N. L. Miller, Comparison of field, laboratory, and theoretical estimates of global nitrogen fixation by lightning, *J. Geophys. Res.*, **95**, D13, 22489-22494, 1990.

Lyons, W. A., Nelson, T. E., Williams, E. R., Cramer, J., Turner, T., Enhanced positive cloud-to-ground lightning in thunderstorms ingesting smoke, *Science*, **282**, 77-81, 1998.

Mach, D. M., H. J. Christian, R. J. Blakeslee, D. J. Boccippio, S. J. Goodman, and W. L. Boeck, Performance assessment of the Optical Transient Detector and Lightning Imaging Sensor, *J. Geophys. Res.*, **112**, D09210, doi:10.1029/2006JD007787, 2007.

Mackerras, D., M. Darveniza, R. E. Orville, E. R. Williams, and S. J. Goodman, Global lightning: total, cloud and ground flash estimates, *J. Geophys. Res.*, **103**, 19791-19809, 1998.

Martin, R. V., D. J. Jacob, and J. A. Logan, Detection of lightning influence on tropical tropospheric ozon*e*, *Geophysical Res. Lett.,* **27**, No. 11, 1639 – 1642, 2000.

Martin, R. V., B. Sauvage, I. Folkins, C. E. Sioris, C. Boone, P. Bernath, and J. R. Ziemke, Space-based constraints on the production of nitric oxide by lightning, *J. Geophys. Res.*, **112**, D09309, doi:10.1029/2006/JD007831, 2007.

Martini, M., D. J. Allen, K. E. Pickering, G. L. Stenchikov, A. Richter, E. J. Hyer, and C. P. Loughner, The impact of North American anthropogenic emissions and lightning on long-range transport of trace gases and their export from the continent during summers 2002 and 2004, *J. Geophys. Res*., **116**, D07305, doi:10.1029/2010JD014305, 2011.

Murray, N. D., Orville, R. E., Huffines, G. R., Effect of pollution from Central American fires on cloud-to-ground lightning in May 1998, *Geophys. Res. Lett.*, **27**, 2249-2252, 2000.

Murray, L. T., D. J. Jacob, J. A. Logan, R. C. Hudman, and W. J. Koshak, Optimized regional and interannual variability of lightning in a global chemical transport model constrained by LIS/OTD satellite data, *J. Geophys. Res.*, **117**, D20307, doi:10.1029/2012JD017934, 2012.

Nesbitt, S. W., R. Zhang, and R. E. Orville, Seasonal and global NO_x production by lightning estimated from the optical Transient Detector (OTD), *Tellus*, **52B**, 1206-1215, 2000.

Newman, M. M., Use of triggered lightning to study the discharge channel. In *Problems of Atmospheric and Space Electricity*, pp. 482-490, New York, Elsevier, 1965.

Noxon, J. F., Atmospheric nitrogen fixation by lightning, *Geophys. Res. Lett.*, **3**, 463-465, 1976.

Noxon, J. F., Tropospheric NO_2, *J. Geophys. Res.*, **83**, 3051-3057, 1978.

Orville, R. E., Huffines, G. R., Nielsen-Gammon, J., Zhang, R., Ely, B., Steiger, S., Phillips, S., Allen, S., Read, W., Enhancement of cloud-to-ground lightning activity over Houston, Texas, *Geophys. Res. Lett.*, **28**, 2597-2600, 2001.

Orville, R. E., and W. Spencer, Global lightning flash frequency, *Mon. Wea. Rev.*, **107**, 934-943, 1979.

Ott, L. E., K. E. Pickering, G. L. Stenchikov, H. Huntrieser, and U. Schumann, Effects of lightning NO_x production during the 21 July European Lightning Nitrogen Oxides Project storm studied with a three-dimensional cloud-scale chemical transport model, *J. Geophys. Res.*, **112**, D05307, doi:10.1029/2006JD007365, 2007.

Ott, L. E., K. E. Pickering, G. L. Stenchikov, D. J. Allen, A. J. DeCaria, B. Ridley, R.F Lin, S. Lang, W. K. Tao, Production of lightning NO_x and its vertical distribution calculated from three-dimensional cloud-scale chemical transport model simulations, *J. Geophys. Res.*, **115,** D04301, doi:10.1-029/2009JD011880, 2010.

Petersen, D., Bailey, M., Beasley, W. H., Hallett, J., A brief review of the problem of lightning initiation and a hypothesis of initial lightning leader formation, **113**, *J. Geophys. Res.*, D17205, doi:10.1029/2007JD009036, 2008.

Peterson, H. S. and W. H. Beasley, Possible catalytic effects of ice particles on the production of NO_x by lightning discharges, *Atmos. Chem. Phys*., **11**, 10259-10268, doi:10.5194/acp-11-10259-2011, 2011.

Peterson, H. S., and J. Hallett, Ice particle growth in the presence of nitric oxide, *J. Geophys. Res.*, **117**, D06302, doi:10.1029/2011JD016986, 2012.

Pickering, K.E., Y.S. Wang, W.K. Tao, C. Price, and J.F. Muller, Vertical distributions of lightning NO_x for use in regional and global chemical transport models, *J. Geophys. Res.*, **103** (D23), 31203-31216, 1998.

Peyrous, R. and R. M. Lapeyre, Gaseous products created by electrical discharges in the atmosphere and condensation nuclei resulting from gaseous phase reactions, *Atmos. Environ.*, **16**, 959-968, 1982.

Price, C. and D. Rind, A simple lightning parameterization for calculating global lightning distributions, *J. Geophys. Res.*, **97**, 9919-9933, 1992.

Price, C. and D. Rind, What determines the cloud-to-ground lightning fraction in thunderstorms?, *Geophys. Res. Lett.*, **20**, No. 6, 463-466, 1993.

Price, C. and D. Rind, Possible implications of global climate change on global lightning distributions and frequencies, *J. Geophys. Res.*, **90**, D5, 10823-10831, 1994.

Price, C., J. Penner, and M. Prather, NO_x from lightning: 1. Global distribution based on lightning physics, *J. Geophys. Res.*, **102**, D5, 5929-5941, 1997.

Price, C., Evidence for a link between global lightning activity and upper tropospheric water vapor, *Nature*, **406**, 290-293, 2000.

Rahman, M., V. Cooray, V. A. Rakov, M. A. Uman, P. Liyanage, B. A. DeCarlo, J. Jerauld, and R. C. Olsen III, Measurements of NO_x produced by rocket-triggered lightning, *Geophys. Res. Lett.*, **34**, L03816, doi:10.1029/2006GL027956, 2007.

Rakov, V. A., M. A. Uman, *Lightning: Physics and Effects*, Cambridge University Press, Cambridge, United Kingdom, ISBN 0 521 583276 6, 687 pp., 2003.

Reeve, N., and R. Toumi, Lightning activity as an indicator of climate change, *Quart. J. Roy. Met. Soc.*, **125**, 893-903, 1999.

Reiter, R., On the causal relation between nitrogen-oxygen compounds in the troposphere and atmospheric electricity, *Tellus*, **22**, 122-135, 1970.

Ridley, B. A., J. E. Dye, J. G. Walega, J. Zheng, F. E. Grahek, and W. Rison, On the production of active nitrogen by thunderstorms over New Mexico, *J. Geophys. Res.*, **101**, 20985-21005, doi:10.1029/96JD01706, 1996.

Ridley, B., L. Ott, K. Pickering, et al., Florida thunderstorms: a faucet of reactive nitrogen to the upper troposphere, *J. Geophys. Res.*, **109**, 1-19, doi:10.1029/2004JD004769, 2004.

Schmidt, G.A., R. Ruedy, J. E. Hansen, et al., Present day atmospheric simulations using GISS ModelE: Comparison to in-situ, satellite and reanalysis data. *J. Climate*, **19**, 153-192, doi:10.1175/JCLI3612.1, 2006.

Schumann, U., H. Huntrieser, H. Schlager, L. Bugliaro, C. Gatzen, and H. Hoeller, Nitrogen oxides from thunderstorms- results from experiments over Europe and the continental tropics, *Deutsch-Österreichisch-Schweizerische Meteorologen-Tagung (DACH)*, Deutsche Meteorologische Gesellschaft, Karlsruhe, Germany, 7-10 September, 2004.

Schumann, U., and H. Huntrieser, The global lightning-induced nitrogen oxides source, *Atmos. Chem. Phys.*, **7**, 3823-3907, 2007.

Shindell, D.T., J. L. Grenfell, D. Rind, V. Grewe, and C. Price, 2001: Chemistry-climate interactions in the Goddard Institute for Space Studies general circulation model: 1. Tropospheric chemistry model description and evaluation. *J. Geophys. Res.*, **106**, 8047-8076, doi:10.1029/2000JD900704, 2001.

Shindell, D.T., G. Faluvegi, and N. Bell, Preindustrial-to-present-day radiative forcing by tropospheric ozone from improved simulations with the GISS chemistry-climate GCM. *Atmos. Chem. Phys.*, **3**, 1675-1702, doi:10.5194/acp-3-1675-2003, 2003.

Shindell, D.T., G. Faluvegi, N. Unger, E. Aguilar, G.A. Schmidt, D.M. Koch, S.E. Bauer, and R.L. Miller, Simulations of preindustrial, present-day, and 2100 conditions in the NASA GISS composition and climate model G-PUCCINI, *Atmos. Chem. Phys.*, **6**, 4427-4459, doi:10.5194/acp-6-4427-2006, 2006.

Shindell, D. T., A. Voulgarakis, G. Faluvegi, and G. Milly, Precipitation response to regional radiative forcing, *Atmos. Chem. Phys. Disc.*, **12**, 5015–5037, 2012.

Sisterson, D. L., and Y. P. Liaw, An evaluation of lightning and corona discharges on thunderstorm air and precipitation chemistry, *J. Atmos. Chem.*, **10**, 83-96, 1990.

Skamarock, W. C., J. G. Powers, M. Barth, J. E. Dye, T. Matejka, D. Bartels, K. Baumann, J. Stith, D. D. Parrish, and G. Hubler, Numerical simulations of the July 10 Stratospheric-Tropospheric Experiment: Radiation, Aerosols, and Ozone – Deep Convection Experiment convective system: Kinematics and transport, *J. Geophys. Res.*, **105**, 19973-19990, 2000.

Skamarock, W. C., J. E. Dye, E. Defer, M. C. Barth, J. L. Stith, B. A. Ridley, and K. Baumann, Observational- and modeling-based budget of lightning-produced NO_x in a continental thunderstorm, *J. Geophys. Res.*, **108**, 4305, doi:10.1029/2002JD002163, 2003.

Sparrow, J. G., and E. P. Ney, Lightning observations by satellite, *Nature*, **232**, 540-541, 1971.

Stavrakou, T., J.-F. Müller, K. F. Boersma, R. J. van der A, J. Kurokawa, T. Ohara, and Q. Zhang, Key chemical NO_x sink undertainties and how they influence top-down emissions of nitrogen oxides, *Atmos. Chem. Phys. Discuss.*, **13**, 7871-7929, 2013.

Steiger, S. M., Orville, R. E., Huffines, G., Cloud-to-ground lightning characteristics over Houston, Texas: 1989-2000, *J. Geophys. Res.*, **107**, doi:10.1029/2001JD001142, 2002.

Stenchikov, G., K. Pickering, A. DeCaria, W.-K. Tao, J. Scala, L. Ott, D. Bartels, and T. Matejka, Simulation of the fine structure of the 12 July 1996 Stratosphere-Troposphere Experiment: Radiation, Aerosols, and Ozone (STERAO-A) storm accounting for the effects of terrain and interaction with mesoscale flow, *J. Geophys. Res.*, **110**, D14304, doi:10.1029/2004JD005582, 2005.

Stith, J., J. Dye, B. Ridley, P. Laroche, E. Defer, K. Baumann, G. Hübler, R. Zerr, and M. Venticinque, NO signatures from lightning flashes, *J. Geophys. Res.*, **104**, 16081-16089, 1999.

Suszcynsky, D. M., M. W. Kirkland, A. R. Jacobson, R. C. Franz, and S. O. Knox, FORTE observations of simultaneous VHF and optical emissions from lightning: Basic phenomenology, *J. Geophys. Res.*, **105**, D2, 2191-2201, 2000.

Suszcynsky, D. M., T. E. Light, S. Davis, J. L. Green, J. L. L. Guillen, and W. Myre, Coordinated observations of optical lightning from space using the FORTE photodiode detector and CCD imager, *J. Geophys. Res.*, **106**, D16, 17897-17906, 2001.

Thomas, R. J., P. R. Krehbiel, W. Rison, S. J. Hunyady, W. P. Winn, T. Hamlin, and J. Harlin, Accuracy of the Lightning Mapping Array, *J. Geophys. Res.*, **109**, D14207, doi:10.1029/2004JD004549, 2004.

Tuck, A. F., Production of nitrogen oxides by lightning discharges, *Q. J. R. Meteor. Soc.*, **102**, 749-755, 1976.

Turman, B. N. and B. C. Edgar, Global lightning distributions at dawn and dusk, *J. Geophys. Res.*, **87**, 1191-1206, 1982.

Uman, M. A., V. A. Rakov, K. J. Rambo, T. W. Vaught, M. I. Fernandez, D. J. Cordier, R. M. Chandler, R. Bernstein, and C. Golden, Triggered-lightning experiments at Camp Blanding, Florida (1993-1995), *Trans. IEE Japan*, **117-B**, 446-452, 1997.

Viemeister, P. E., Lightning and the origin of nitrates found in precipitation, *J. Meteor.*, **17**, 6811-683, 1960.

Visser, S., Chemical composition of rain water in Kampala, Uganda, and its relation to meteorological and topographical conditions, *J. Geophys. Res*., **66**, 3759-3765, 1961.

Von Liebig, J., Une note sur la nitrification, *Ann. Chem. Phys.*, **35**, 329-333, 1827.

Vorpahl, J. A., J. G. Sparrow, and E. P. Ney, Satellite observations of lightning, *Science*, **169**, 860-862, 1970.

Wang, Y., A. W. DeSilva, and G. C. Goldenbaum, Nitric oxide production by simulated lightning: dependence on current, energy, and pressure, *J. Geophys. Res.*, **103**, 19149-19159, 1998.

Waters, J. W., et al., The Earth Observing System Microwave Limb Sounder (EOS MLS) on the Aura satellite, *IEEE Trans. Geosci. Remote Sens.*, **44**, 1075-1092, doi:10.1109/TGRS.2006.8, 2006.

Williams, E. R., T. Chan, and D. Boccippio, Islands as miniature continents: another look at the land-ocean lightning contrast, *J. Geophys. Res.*, **109**, D16206, 2004.

Williams, E. R., Lightning and climate: a review, *Atmo. Res.*, **76**, 272-287, 2005.

Zhang, X., J. H. Helsdon Jr., and R. D. Farley, Numerical modeling of lightning-produced NO_x using an explicit lightning scheme: 1. Two-dimensional simulation as a 'proof of concept', *J. Geophys. Res*., **108**, D18, 4579, doi:10.1029/2002JD003224, 2003.

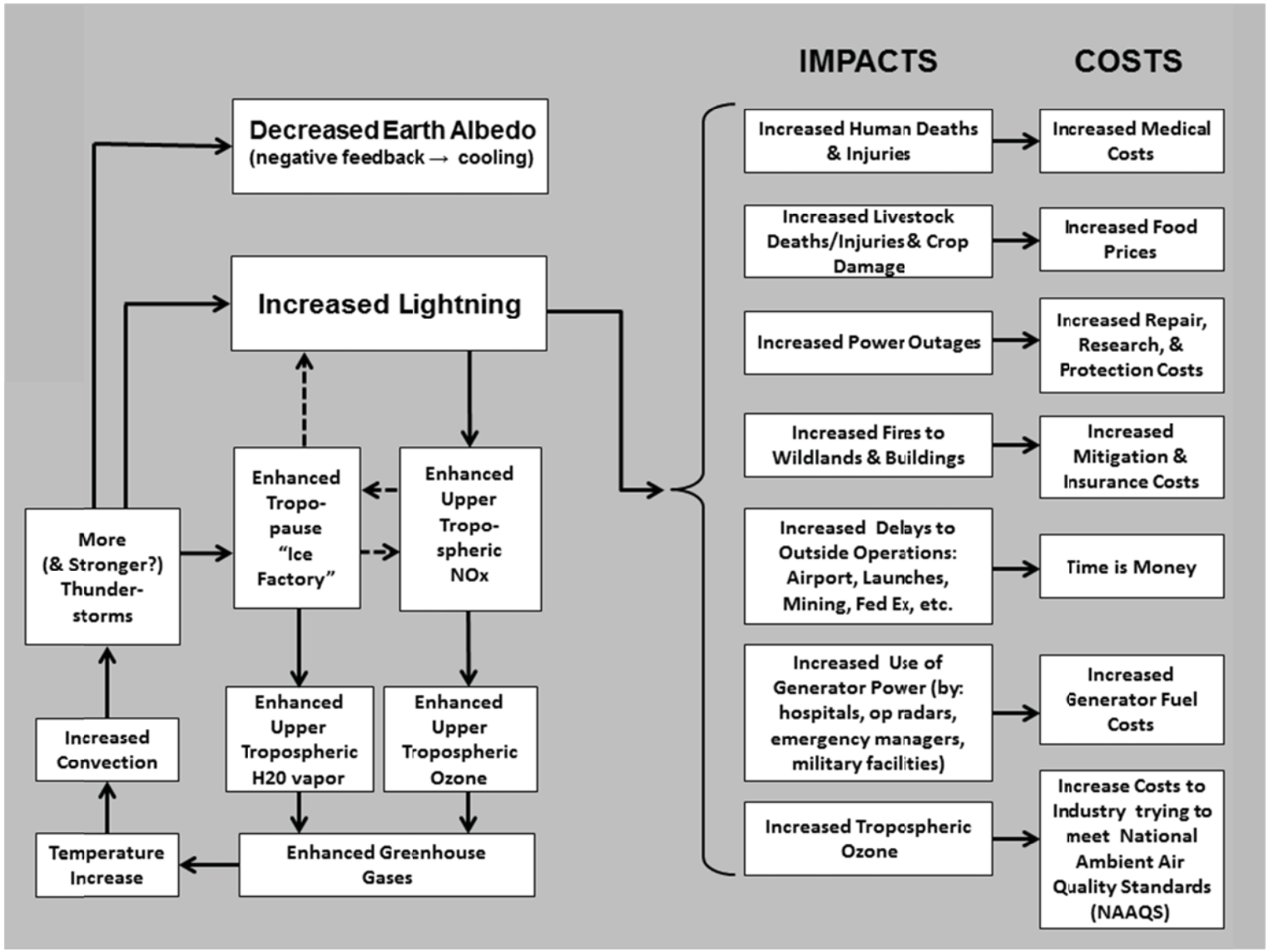

Figure 5.1 Overview of many important impacts of lightning, and the central role played by lightning nitrogen oxides.

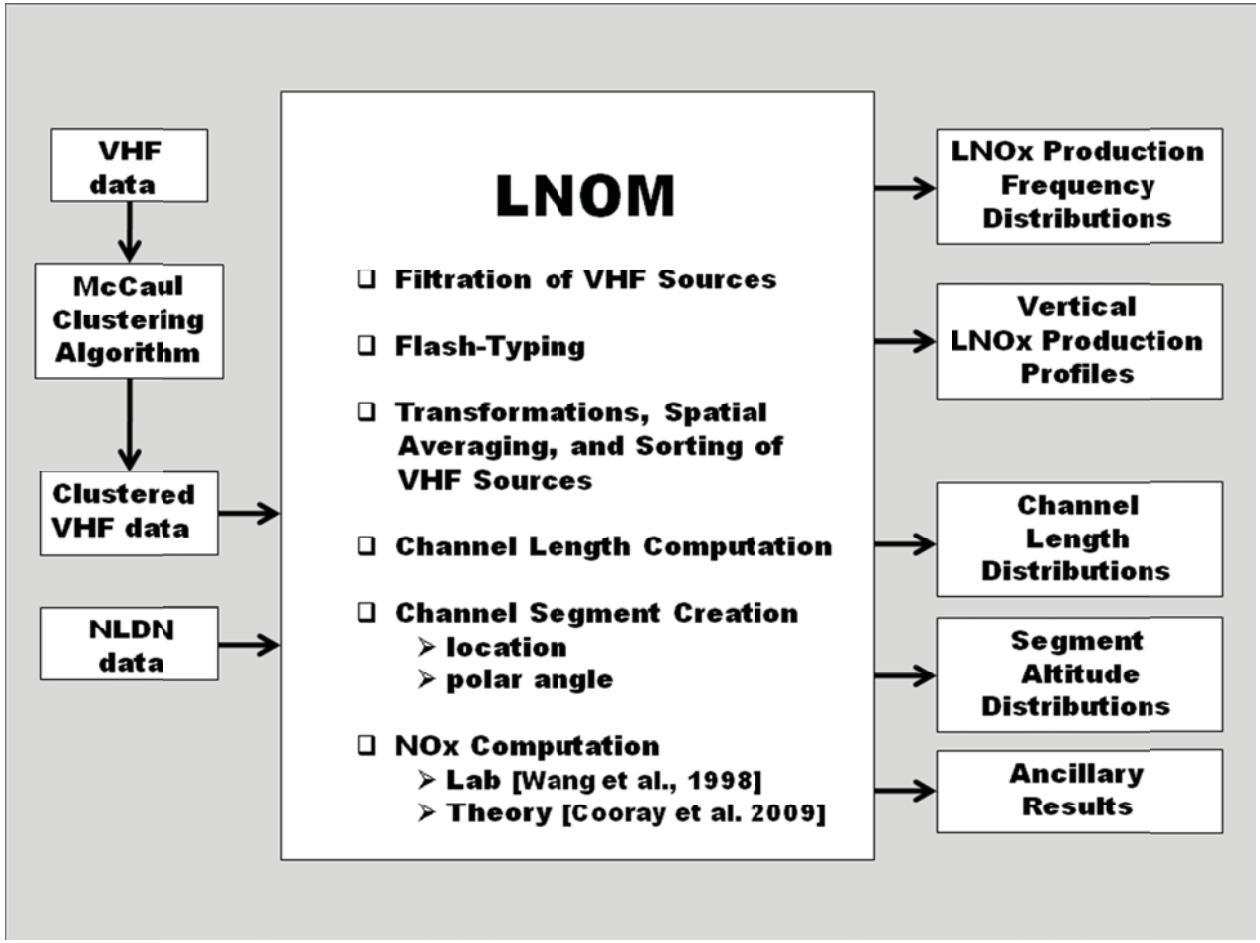

Figure 5.2 The LNOM ingests 4D VHF lightning channel mapping data and NLDN data to obtain the products shown on the right side of the flow diagram. These products are produced for ground flashes, for cloud flashes, and for all flashes.

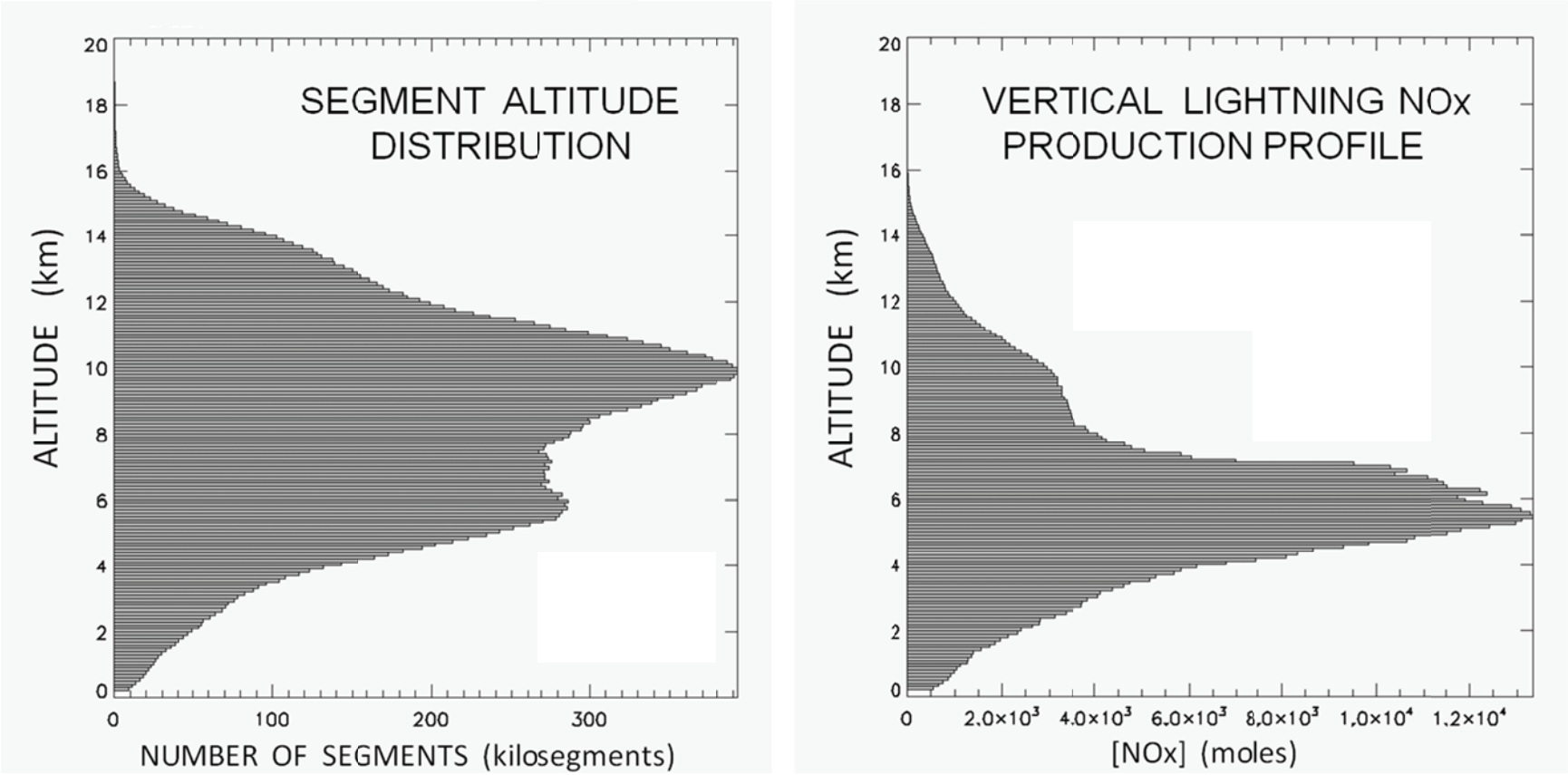

Figure 5.3 Examples of altitude dependent LNOM products: SAD (left), and LNPP (right) for an August 2006 air quality study [adapted from Koshak et al., 2013].

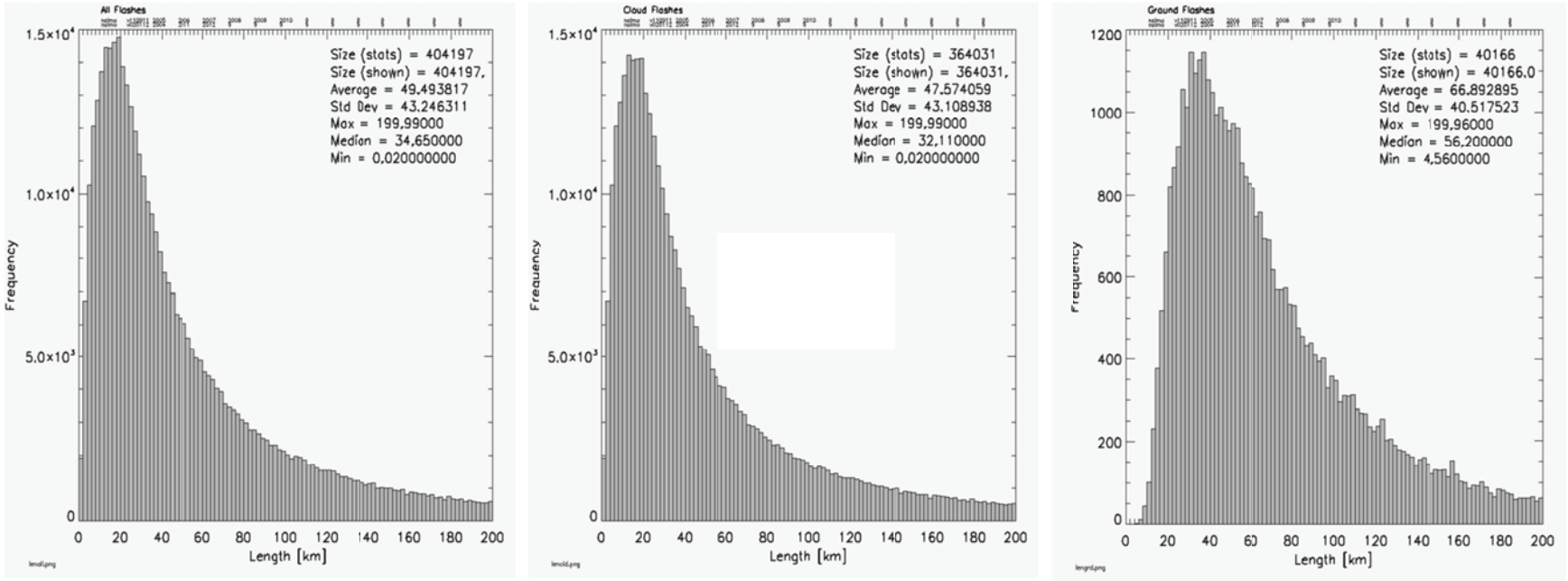

Figure 5.4 The LNOM-derived frequency distributions of lightning channel lengths for: all flashes (left), cloud flashes (middle), and ground flashes (right). These results are for 9 years (2004-2012) of North Alabama thunderstorms.

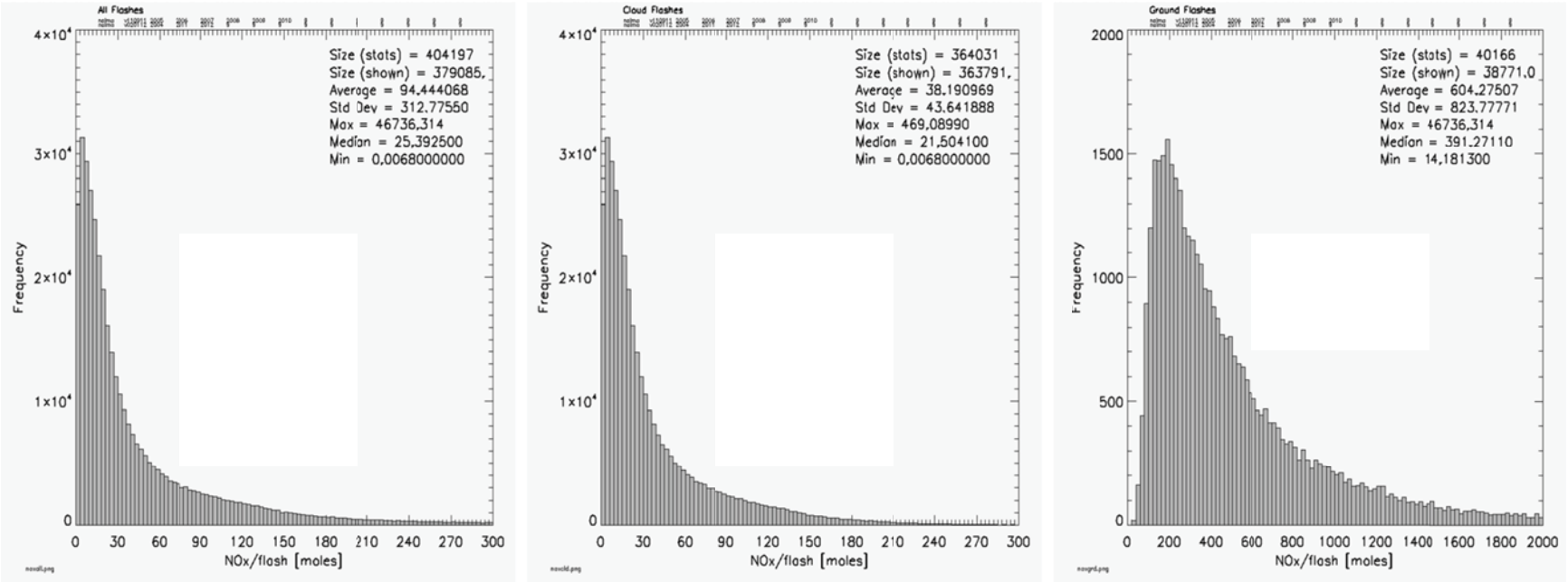

Figure 5.5 The LNOM-derived frequency distributions of flash LNOx for: all flashes (left), cloud flashes (middle), and ground flashes (right). These results are for 9 years (2004-2012) of North Alabama thunderstorms.

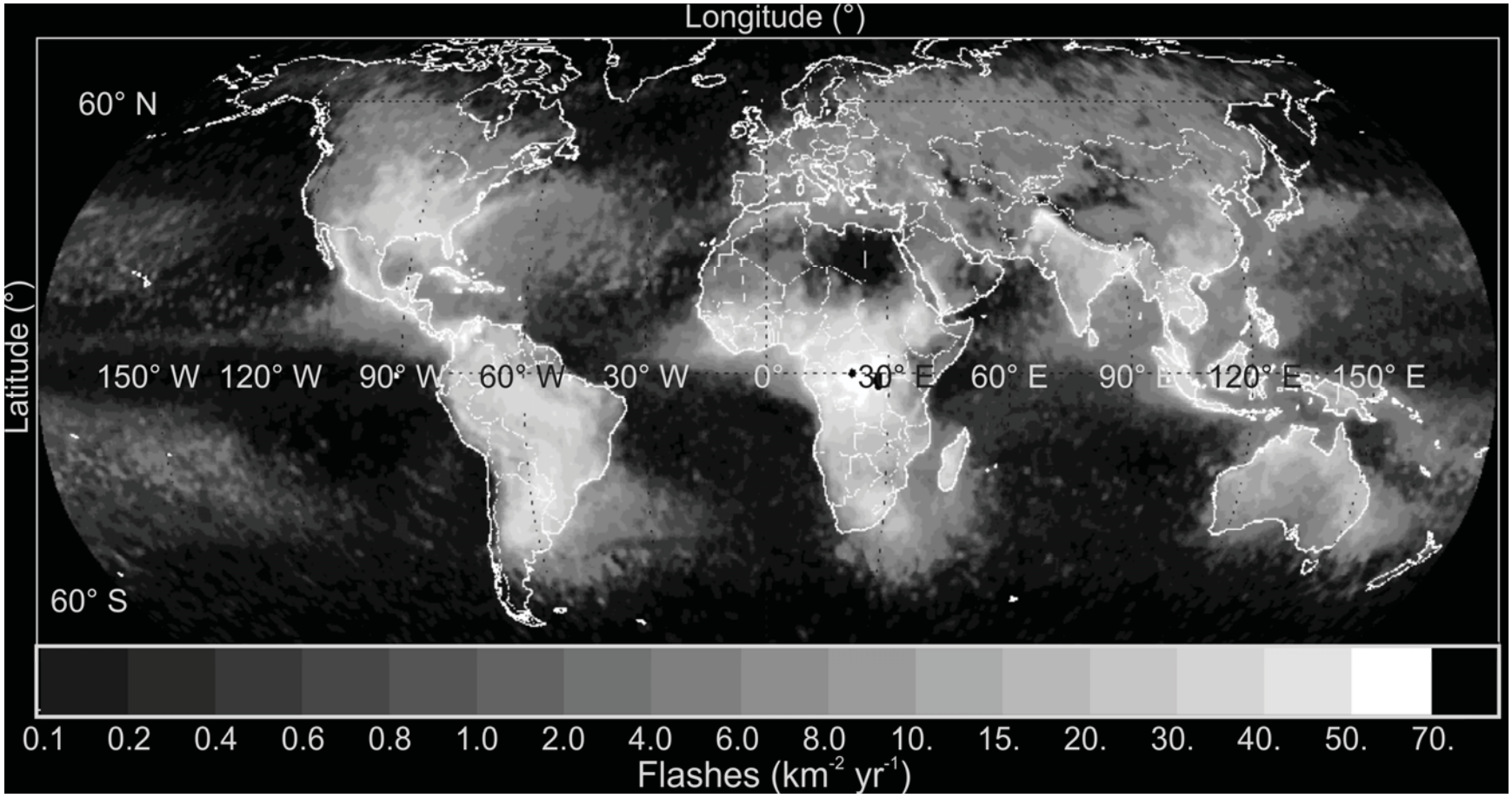

Figure 5.6 The global annual flash density (flashes km^{-2} yr^{-1}) distribution based on OTD and LIS data [adapted from Mach et al., 2007].

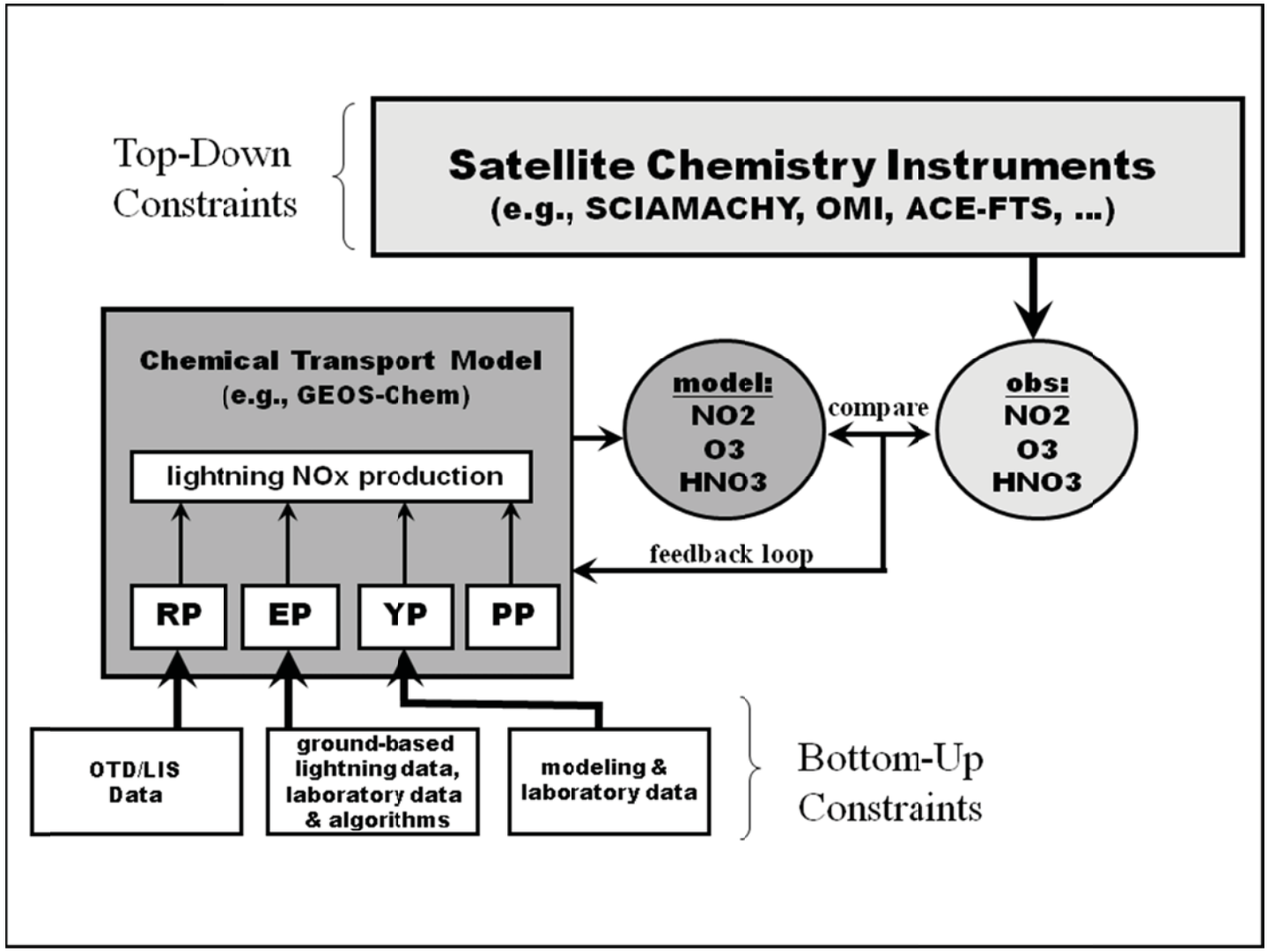

Figure 5.7 An example of optimizing various lightning parameterizations within a model to best fit satellite chemistry measurements (see main text for description of variables shown).

Table 5.2 Lightning NO production inferred from a simple plume model [as provided in Table 1 of Stith et al., 1999].

Date	Time of Peak (GMT)	NO Peak, ppbv	Pressure, Pa	Plume Mean NO, ppbv	Plume s.d.,* ppbv	Back-ground Mean NO, ppbv	Back-ground s.d., ppbv	Mean NO Above Background, ppbv	Plume Diameter, m	Tempera-ture, °C	NO Produced, molecules m^{-1}	Spike Category (See Text)
July 9	2332:55	1.70	40900	1.03	0.43	0.29	0.08	0.74	753	−17	3.8E + 21	A
	2333:07	1.40	40900	1.00	0.33	0.34	0.05	0.66	452	−17	1.2E + 21	A
	2333:27	1.80	40100	1.40	0.56	0.65	0.07	0.75	228	−16	3.5E + 20	A
	2333:39	4.50	40900	4.47		0.95	0.16	3.52	110	−16	3.9E + 20	A
	2334:42	4.30	40100	4.32		0.86	0.28	3.46	110	−17	3.7E + 20	A
	2334:46	18.70	40100	11.58	7.55	0.86	0.28	10.72	330	−17	1.0E + 22	A
	2334:50	15.00	40100	8.73	8.88	0.86	0.28	7.87	220	−17	3.4E + 21	A
	2335:29	6.85	41300	2.40	2.98	0.55	0.19	1.85	464	−17	3.7E + 21	A
	2335:31	8.00	41300	6.58	2.01	0.55	0.19	6.03	232	−17	3.0E + 21	A
	2335:39	2.40	41200	2.42		0.73	0.15	1.69	114	−17	2.0E + 20	A
July 10	2249:54	0.83	24000	0.59	0.33	0.13	0.02	0.46	278	−47	2.1E + 20	C
	2259:47	0.79	21700	0.57	0.20	0.21	0.04	0.36	407	−52	3.3E + 20	B
	2307:44	4.20	20900	2.55	0.93	1.17	0.16	1.38	964	−54	7.0E + 21	B
	2348:44	0.60	23900	0.34	0.19	0.05	0.02	0.29	673	−47	7.9E + 20	B
Mean									3.8E + 02		2.5E + 21	

Read 3.8E + 21 as 3.8×10^{21}.
*Standard deviations (s.d.) are omitted for plumes 1 s long.